(12) INTERNATIONAL APPLICATION PUBLISHED UNDER THE PATENT COOPERATION TREATY (PCT)

(19) **World Intellectual Property Organization**
International Bureau

(43) **International Publication Date**
22 August 2024 (22.08.2024)

WIPO | PCT

(10) **International Publication Number**
WO 2024/171093 A1

(51) **International Patent Classification:**
H04B 7/04 (2017.01) *H04B 7/06* (2006.01)

(21) **International Application Number:**
PCT/IB2024/051409

(22) **International Filing Date:**
15 February 2024 (15.02.2024)

(25) **Filing Language:** English

(26) **Publication Language:** English

(30) **Priority Data:**
23156936.9 15 February 2023 (15.02.2023) EP

(71) **Applicant: POLITECNICO DI MILANO** [IT/IT]; Piazza Leonardo da Vinci, 32, 20133 Milano (IT).

(72) **Inventors: SPAGNOLINI, Umberto**; c/o Politecnico di Milano, Piazza Leonardo da Vinci, 32, I-20133 Milano (IT). **TAGLIAFERRI, Dario**; c/o Politecnico di Milano, Piazza Leonardo da Vinci, 32, I-20133 Milano (IT). **MIZMIZI, Marouan**; Piazza Bande Nere, 9, I-20146 Milano (IT).

(74) **Agent: CARUTI, Filippo** et al.; c/o THINX S.r.l., Piazzale Luigi Cadorna, 10, 20123 Milan (IT).

(81) **Designated States** *(unless otherwise indicated, for every kind of national protection available)*: AE, AG, AL, AM, AO, AT, AU, AZ, BA, BB, BG, BH, BN, BR, BW, BY, BZ, CA, CH, CL, CN, CO, CR, CU, CV, CZ, DE, DJ, DK, DM, DO, DZ, EC, EE, EG, ES, FI, GB, GD, GE, GH, GM, GT, HN, HR, HU, ID, IL, IN, IQ, IR, IS, IT, JM, JO, JP, KE, KG, KH, KN, KP, KR, KW, KZ, LA, LC, LK, LR, LS, LU, LY, MA, MD, MG, MK, MN, MU, MW, MX, MY, MZ, NA, NG, NI, NO, NZ, OM, PA, PE, PG, PH, PL, PT, QA, RO, RS, RU, RW, SA, SC, SD, SE, SG, SK, SL, ST, SV, SY, TH, TJ, TM, TN, TR, TT, TZ, UA, UG, US, UZ, VC, VN, WS, ZA, ZM, ZW.

(84) **Designated States** *(unless otherwise indicated, for every kind of regional protection available)*: ARIPO (BW, CV, GH, GM, KE, LR, LS, MW, MZ, NA, RW, SC, SD, SL, ST, SZ, TZ, UG, ZM, ZW), Eurasian (AM, AZ, BY, KG, KZ, RU, TJ, TM), European (AL, AT, BE, BG, CH, CY, CZ, DE, DK, EE, ES, FI, FR, GB, GR, HR, HU, IE, IS, IT, LT, LU, LV, MC, ME, MK, MT, NL, NO, PL, PT, RO, RS, SE,

(54) **Title:** WIRELESS COMMUNICATIONS WITH SPACE-TIME MODULATED METASURFACES

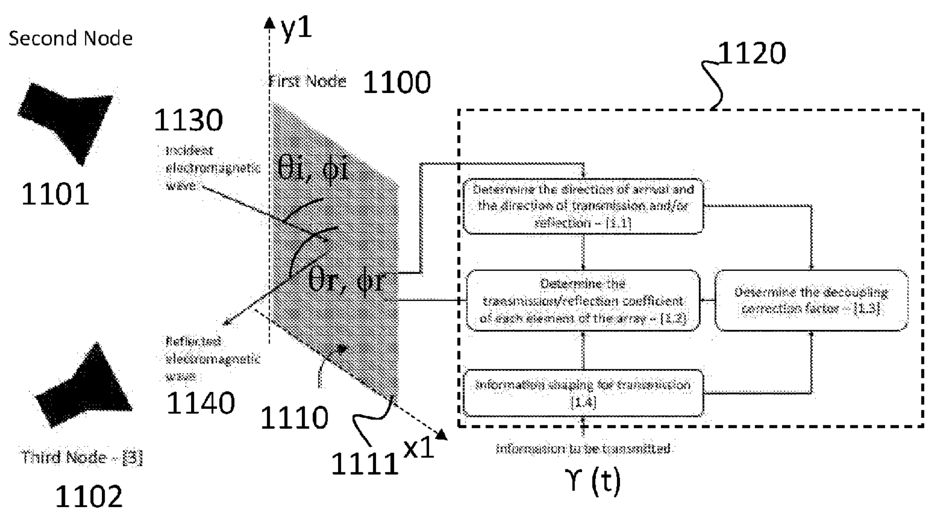

Fig. 2

(57) **Abstract:** A wireless communication device comprising an array (110) of reflective elements (111) adapted to reflect an incident electromagnetic wave (130), and a control unit (120) operatively connected to each reflective element of the array in order to space-time modulating the incident electromagnetic wave to transmit additional information with the reflected electromagnetic wave (140). The control unit is configured to control each reflective element in order to introduce, in the incident electromagnetic wave that hits the reflective element, a phase shift which depends (i) on the additional information to be transmitted, (ii) on the incident angles Θ_i and Φ_i formed between the plane on which the array rests and the incident electromagnetic wave, (iii) on the reflection angle Θ_r and Φ_r formed between the plane on which the array rests and the reflected electromagnetic wave, and (iv) on the space distance between the reflective elements.

WO 2024/171093 A1

[Continued on next page]

SI, SK, SM, TR), OAPI (BF, BJ, CF, CG, CI, CM, GA, GN, GQ, GW, KM, ML, MR, NE, SN, TD, TG).

Declarations under Rule 4.17:
— *of inventorship (Rule 4.17(iv))*

Published:
— *with international search report (Art. 21(3))*

WIRELESS COMMUNICATIONS WITH SPACE-TIME MODULATED METASURFACES

TECHNICAL FIELD

The present invention relates to devices for wireless communication, in particular to metasurfaces operated to add information data to a received electromagnetic signal and reflect/transmit the received signal with the additional information data in a predetermined direction.

BACKGROUND ART

The development of future wireless communication networks is a collective effort that entails the integration of multiple technologies as well as addressing several challenges. The goal of 6G is to provide ultra-high data rates, low latency, and high reliability for a wide range of applications and services such as autonomous vehicles, eHealth, and the Internet of Things [1], [2]. To reach these objectives, 6G links must integrate advanced technologies with the use of high-frequency bands and energy-efficient solutions.

The emergence of electromagnetic (EM) metasurfaces, a.k.a. reconfigurable intelligent surfaces (RIS), has opened up new possibilities in the design of wireless propagation [3]. A RIS, illustrated in Figure 1a, is typically made of quasi-passive arrays of sub-wavelength-sized elements whose scattering properties are engineered to manipulate the impinging EM waves and control the reflection [4].

RIS underwent tremendous conceptual and, to a minor extent, experimental development through several studies. In particular, RISs have been proposed for overcoming blockage [5], with specific application to vehicular scenarios [6]–[8], for coverage extension [9] and, recently, as support for sensing [10], [11].

The RIS technology (and metamaterials in general) has experienced a surge in interest in the last decade, following the formulation of the generalized Snell's law in 2011 [12]. It is based on the conservation of both the linear momentum and the energy of reflected and refracted waves [13]. The linear momentum is related to spatial symmetry, i.e., an EM wave impinging from an arbitrary angle θi is reflected at the specular one $\theta o = \theta i$. Setting the spatial-phase gradient across the RIS implies breaking the spatial symmetry, thus allowing a reflection toward an angle $\theta o \neq \theta i$.

Energy conservation relates to the time-reversal symmetry or Lorentz reciprocity, i.e., if one can reflect an EM wave coming from a particular angle θi towards a specific angle θo, the same EM wave coming back from θo will be reflected toward θi.

In 2014, in [14] it is proposed the universal Snell's law of reflection for realizing efficient solar panels, while [15] discloses a first application for solar panels. The key idea is to break the energy conservation law – due to the frequency shift imposed by the metasurface modulating the incident EM wave – by adding a temporal phase gradient across the metasurface and then combining the spatial and temporal phase gradients in the metasurface to create anomalous nonreciprocal reflections. This principle is at the foundation of space-time modulated metasurfaces (STMMs) and generalizes RISs, opening up the possibility of conveying information in the reflected EM waves [16].

Figures 1a, 1b and 1c depicts the evolution of metasurfaces from RIS (Figure 1a) to STCM (Figure 1b) and STMM (Figure 1c).

As explained above, through a RIS 100 a wave 101, transmitted at frequency f_c and impinging the surface at angle θi, can be reflected at angle θo ≠ θi. The reflected wave 102 maintains the same frequency f_c of the impinging wave.

The authors in [17]–[19] used a spatial-temporal gradient to create space-time coded metasurfaces (STCMs), which can both reflect the signal in space and shift its frequency, generating harmonics. As illustrated in Figure 1b, STCM 110 can be programmed to reflect a wave 101, having frequency fc and impinging the angle θi, in desired directions and with desired frequency. In Figure 1b, three different reflected waves are illustrated. Reflected wave 102 has same frequency fc of the impinging wave 101, but different angle with respect to the STCM 110. Reflected wave 103 has frequency f_c-f_m, and reflected wave 104 has frequency f_c+f_m, f_m being a frequency shift introduced by the STCM.

STMMs differ from STCMs in that they are intended to convey information through reflection, whereas STCMs are primarily designed to synthesize time-varying reflection patterns. As illustrated in Figure 1c, an electric signal, carrying Data B at the same frequency f_c of the impinging wave 101, is applied to the STMM 120 and the information is added to Data A carried by wave 101 in the reflected wave 106.

The work in [20] proposes a STMM-based MIMO transmitter that operates on a sinusoidal feed and encodes data using the harmonics of a properly designed phase-discontinuous symbol. However, the interaction between spatial and temporal phases is not investigated. Nevertheless, the theoretical findings of [20] are validated by experimental results in a 2 × 2 MIMO setting, demonstrating a rate of 20 Mbps. The authors of [21] discuss the realization of advanced modulation schemes by engineering the phase response of the single STMM element. From a system-level perspective, the work in [22] describes an STMM-based beamforming-plus-phase modulation system to serve a user with information augmentation, focusing on beamforming and detection performance. The authors in [23] propose to enhance ambient backscatter communications with a phase-modulated STMM. The authors consider a binary phase shift keying (BPSK) modulation scheme and derive the spectral efficiency of the system in a quasi-stationary condition (i.e., without considering the effects of the temporal and spatial phase gradients coupling on the performance).

REFERENCES

[1] W. Saad, M. Bennis, and M. Chen, "A vision of 6G wireless systems: Applications, trends, technologies, and open research problems," IEEE Network, vol. 34, no. 3, pp. 134–142, 2020.

[2] M. Mizmizi, M. Brambilla, D. Tagliaferri, C. Mazzucco, M. Debbah, T. Mach, R. Simeone, S. Mandelli, V. Frascolla, R. Lombardi et al., "6g v2x technologies and orchestrated sensing for autonomous driving," arXiv preprint arXiv:2106.16146, 2021.

[3] M. Di Renzo, A. Zappone, M. Debbah, M.-S. Alouini, C. Yuen, J. De Rosny, and S. Tretyakov, "Smart radio environments empowered by reconfigurable intelligent surfaces: How it works, state of research, and the road ahead," IEEE Journal on Selected Areas in Communications, vol. 38, no. 11, pp. 2450–2525, 2020.

[4] Y. Zhang, J. Zhang, M. Di Renzo, H. Xiao, and B. Ai, "Performance analysis of ris-aided systems with practical phase shift and amplitude response," IEEE Transactions on Vehicular Technology, 2021.

[5] L. Jiao, P. Wang, A. Alipour-Fanid, H. Zeng, and K. Zeng, "Enabling efficient blockage-aware handover in ris-assisted mmwave cellular networks," IEEE Transactions on Wireless Communications, pp. 1–1, 2021.

[6] M. Mizmizi, R. A. Ayoubi, D. Tagliaferri, K. Dong, G. G. Gentili, and U. Spagnolini, "Conformal metasurfaces: a novel solution for vehicular communications," IEEE Transactions on Wireless Communications, pp. 1–1, 2022.

[7] D. Tagliaferri, M. Mizmizi, R. A. Ayoubi, G. G. Gentili, and U. Spagnolini, "Conformal intelligent reflecting surfaces for 6g v2v communications," in 2022 1st International Conference on 6G Networking (6GNet), 2022, pp. 1–8.

[8] M. Mizmizi, D. Tagliaferri, M. Khosronejad, L. Resteghini, G. G. Gentili, L. Draghi, and U. Spagnolini, "Conformal metasurfaces for recovering dynamic blockage in vehicular systems," in GLOBECOM 2022 - 2022 IEEE Global Communications Conference, 2022, pp. 6025–6030.

[9] Y. U. Ozcan, O. Ozdemir, and G. K. Kurt, "Reconfigurable intelligent surfaces for the connectivity of autonomous vehicles," IEEE Transactions on Vehicular Technology, vol. 70, no. 3, pp. 2508–2513, 2021.

[10] S. Buzzi, E. Grossi, M. Lops, and L. Venturino, "Radar target detection aided by reconfigurable intelligent surfaces," IEEE Signal Processing Letters, vol. 28, pp. 1315–1319, 2021.

[11] S. Buzzi, E. Grossi, M. Lops, L. Venturino , "Foundations of mimo radar detection aided by reconfigurable intelligent surfaces," IEEE Transactions on Signal Processing, vol. 70, pp. 1749–1763, 2022.

[12] N. Yu, P. Genevet, M. A. Kats, F. Aieta, J.-P. Tetienne, F. Capasso, and Z. Gaburro, "Light propagation with phase discontinuities: Generalized laws of reflection and refraction," Science, vol. 334, no. 6054, pp. 333–337, 2011. [Online]. Available: https://www.science.org/doi/abs/10.1126/science.1210713

[13] A. Shaltout, A. Kildishev, and V. Shalaev, "Time-varying metasurfaces and lorentz non-reciprocity," Optical Materials Express, vol. 5, no. 11, pp. 2459–2467, 2015.

[14] L. Zhang, X. Q. Chen, S. Liu, Q. Zhang, J. Zhao, J. Y. Dai, G. D. Bai, X. Wan, Q. Cheng, G. Castaldi, V. Galdi, and T. J. Cui, "Space-time-coding digital metasurfaces," Nature Communications, vol. 9, no. 1, p. 4334, Oct 2018.

[15] Y. Hadad, J. C. Soric, and A. Alu, "Breaking temporal symmetries for emission and absorption," Proceedings of the National Academy of Sciences, vol. 113, no. 13, pp. 3471–3475, 2016.

[16] S. Taravati and G. V. Eleftheriades, "Microwave space-time-modulated metasurfaces," ACS Photonics, vol. 9, no. 2, pp. 305–318, 2022.

[17] Zhang, Lei, Dai, Jun Yan, Moccia, Massimo, Castaldi, Giuseppe, Cui, Tie Jun, and Galdi, Vincenzo, "Recent advances and perspectives on space-time coding digital metasurfaces," EPJ Appl. Metamat., vol. 7, p. 7, 2020. [Online]. Available: https://doi.org/10.1051/epjam/202000728

[18] L. Zhang and T. Cui, "Space-time-coding digital metasurfaces: Principles and applications," Research, vol. 2021, pp. 1–25, 05 2021.

[19] G.-B. Wu, J. Dai, Q. Cheng, T. Cui, and C. Chan, "Sideband-free space–time-coding metasurface antennas," Nature Electronics, vol. 5, no. 11, p. 808–819, Nov. 2022.

[20] W. Tang, J. Y. Dai, M. Z. Chen, K.-K. Wong, X. Li, X. Zhao, S. Jin, Q. Cheng, and T. J. Cui, "Mimo transmission through reconfigurable intelligent surface: System design, analysis, and implementation," IEEE Journal on Selected Areas in Communications, vol. 38, no. 11, pp. 2683–2699, 2020.

[21] J. Y. Dai, W. Tang, L. X. Yang, X. Li, M. Z. Chen, J. C. Ke, Q. Cheng, S. Jin, and T. J. Cui, "Realization of multi-modulation schemes for wireless communication by time-domain digital coding metasurface," IEEE Transactions on Antennas and Propagation, vol. 68, no. 3, pp. 1618–1627, 2020.

[22] S. Lin, F. Chen, M. Wen, Y. Feng, and M. Di Renzo, "Reconfigurable intelligent surface-aided quadrature reflection modulation for simultaneous passive beamforming and information transfer," IEEE Transactions on Wireless Communications, vol. 21, no. 3, pp. 1469–1481, 2022.

[23] S. Y. Park and D. In Kim, "Intelligent reflecting surface-aided phase-shift backscatter communication," in 2020 14th International Conference on Ubiquitous Information

Management and Communication (IMCOM), 2020, pp. 1–5.

OBJECTS AND BRIEF DESCRIPTION OF THE INVENTION

An object of the invention is to solve the problem of the prior art related to reflection or transmission of signals using metasurfaces.

It is an object of the invention to present a solution to transmit information with low costs devices, in particular using metasurfaces.

Embodiments of the present invention comprises two architectures – based on a novel mathematical model for the design of STMMs in wireless communication systems - where the spatial component of the modulation controls the direction in which the signal is reflected, and the temporal component conveys information in the designated direction, specifically in the context of a full-duplex system architecture, which is one of the promising solutions where STMMs can be beneficial.

The full-duplex system architecture comprises a master unit (MU) that transmits a downlink MU→ SU signal and a slave unit (SU) that can receive, reflect, and modulate the MU→SU using STMM technology. In order to transmit information in uplink MU←SU, the SU modulates the temporal phase gradient applied to the metasurface elements. To validate the analytical findings, numerical results are presented, demonstrating the efficacy of the proposed model and its potential to revolutionize wireless communication. These and other objects of the present invention are achieved by wireless communication devices and methods for transmitting information in a wireless network according incorporating the features of the appended claims, which form an integral part of the present description.

According to a first aspect, the present invention is directed to a wireless communication device comprising an array of reflective elements adapted to reflect an incident electromagnetic wave, and a control unit operatively connected to each reflective element of the array to space-time modulating the incident electromagnetic wave to transmit additional information with the reflected electromagnetic wave. The control unit is configured to control each reflective element in order to introduce, in the incident electromagnetic wave that hits the reflective element, a phase shift which depends on the additional information to be transmitted, on the incident angles θ_i and ϕ_i formed between a plane on which the array rests and the incident electromagnetic wave, on the reflection angles θ_r and ϕ_r formed between the plane on which the array rests and the reflected electromagnetic wave, and on the space distance between the reflective elements.

According to a second aspect, the present invention is directed to a wireless communication device comprising an array of transmitting elements adapted to transmit an incident electromagnetic wave, and a control unit operatively connected to each transmitting element of the array to space-time modulating the incident electromagnetic wave to transmit additional information with the transmitted electromagnetic wave. The control unit is configured to control each transmitting element in order to introduce, in the incident electromagnetic wave that hits the transmitting element, a phase shift which depends on the additional information to be transmitted, on the incident angles θ_i and ϕ_i formed between a plane on which the array rests and the incident electromagnetic wave, on the transmission angles θ_t and ϕ_t formed between the plane on which the array rests and the transmitted electromagnetic wave, and on the space distance between the transmitting elements.

According to a third aspect, the present invention is directed to a method for transmitting information in a wireless network. The method comprises the following steps. Determine the incident angle of an incident electromagnetic wave, the incident electromagnetic wave hitting a plurality of reflecting elements of a reflecting surface. Determine the reflection angle of a reflected wave, the reflected electromagnetic wave being transmitted by the plurality of reflecting elements being hit by the incident electromagnetic wave. Acquire an information to be added to the incident electromagnetic wave. Control each reflecting element of the reflective surface in order to introduce, in the incident electromagnetic wave that hits the reflective element, a phase (and amplitude) shift which depends on the additional information to be transmitted, on the incident angles θ_i and ϕ_i formed between the plane on which the array rests and the incident electromagnetic wave, on the reflection angles θ_r and ϕ_r formed between the plane on which the array rests and the reflected electromagnetic wave, and on the space distance between the reflective elements.

According to a fourth aspect, the present invention is directed to a method for transmitting information in a wireless network comprising the following steps. Determine the incident angle of an incident electromagnetic wave, the incident electromagnetic wave hitting a plurality of transmittive elements of a transmitting surface. Determine the transmission angle of a transmitted wave, the transmitted electromagnetic wave being transmitted by the plurality of transmitting elements being hit by the incident electromagnetic wave. Acquire an information to be added to the incident electromagnetic wave. Control each transmitting elements of the array in order to modify the phase of the incident electromagnetic wave by adding a phase shift which depends on the information that the control units is requested to add, on the incident angles θ_i and ϕ_i and the transmission angle θ_t and ϕ_t, and on the space distance between the transmitting elements.

According to a fifth aspect, the present invention is directed to a wireless communication network comprising at least one communication device according to the previous first and second aspects and/or at least one communication device adapted to operate according to the methods of the third and fourth aspect of the invention.

These and other objects of the present invention are achieved by a system incorporating the features of the appended claims, which form an integral part of the present description.

BRIEF DESCRIPTION OF THE DRAWINGS

The invention is described hereinbelow with reference to certain examples provided by way of non-limiting example and illustrated in the accompanying drawings. These drawings illustrate different aspects and embodiments of the present invention and reference numerals illustrating structures, components, materials and/or similar elements in different drawings are indicated by similar reference numerals, where appropriate. Moreover, for clarity of illustration, certain references may not be repeated in all drawings.

Figure 1a shows a RIS metasurface controlling the direction of reflection of an impinging wave,

Figure 1b shows a STCM metasurface controlling direction of reflection and reflected frequency,

Figure 1c shows a wave, carrying information A, impinging on a STMM metasurface which adds information B into the reflected signal.

Figure 2 is a schematic diagram of a wireless communication network comprising a communication device according to a first embodiment of the present invention,

Figure 3a is a schematic side view of a one-dimensional plane wave impinging on a STMM metasurface having a first architecture comprising a spacetime phase shifter for each element according to an embodiment of the present invention,

Figure 3b is a schematic side view of a one-dimensional plane wave impinging on a STMM metasurface having a second architecture comprising a shared temporal phase shifter according to a further embodiment of the invention,

Figure 4a is a schematic cross-sectional side view of a STMM according to an embodiment of the invention, that groups the space-time shifters into partial partitioning, being impinged by one dimensional plane wave,

Figure 4b is a schematic top view of the STMM of Figure 4a,

Figure 5 is a schematic diagram of a wireless communication network comprising a communication device according to a second embodiment of the invention,

Figure 6 shows a two-dimensional STTM reflecting an impinging wave,

Figure 7a is a schematic diagram of a system according to an embodiment of the present invention,

Figure 7b is a schematic isometric view of a metasurface of the system of Figure 7a, showing geometric parameters characterizing impinging and reflected waves,

Figure 8 is a diagram of a normalized reflection gain as a function of space-time phase gradients coupling of a metasurface according to an embodiment of the invention.

Figure 9 is a diagram of an angle of maximum reflection $\tilde{\theta}_0$ as a function of incidence angles θ_i and M=100,

Figure 10 is a diagram of an angle of maximum reflection $\tilde{\theta}_0$as a function of a frequency shift κ and of an incidence angle θ_i (M_u = 100),

Figure 11a is a diagram of a spectral efficiency as a function of SNR at the antenna of the SU in MU $\rightarrow$ SU, for different MU arrays configuration (N = 16$\times$4, 24$\times$16) having various design parameters according to embodiments of the present invention,

Figure 12b is a diagram of a spectral efficiency as a function of MU SU distance, for different MU arrays configuration (N = 16$\times$4, 24$\times$16) having various design parameters according to embodiments of the present invention,

Figure 12c is a diagram of a spectral efficiency as a function of a STMM size for different MU arrays configuration (N = 16$\times$4, 24$\times$16) having various design parameters according to embodiments of the present invention,

Figure 12a and 12b is a diagram of a spectral efficiency considering different metasurface sizes, i.e., M_u = 100 × 100 and M_u = 200 × 200, and different incident angles varying the κ, which is proportional to the MU $\leftarrow$ SU bandwidth B_u, and

Figure 13 is a diagram of the total spectral efficiency as a function the MU$\rightleftarrows$SU bandwidths ratio μ for different metasurface sizes, i.e., M = 100$\times$100 and M = 200$\times$200, and different distances,

DETAILED DESCRIPTION OF THE INVENTION

The state of the art in the field metasurfaces, particularly of STCMs/STMMs, comprises several physical realizations. By generalizing the RIS principle, this document aims to demonstrate the technical features and advantages provided by an STMM-based wireless communication system according to an embodiment of the invention.

Herein, it is considered a master unit (MU), for example, a base station (BS), and a slave unit (SU), e.g., user equipment (UE), in a generic full-duplex system (MU SU). A phase control of STMM enables the superposition of an impinging signal from the slave unit to the master unit – also indicated in the following as MU $\leftarrow$ SU signal, while a corresponding communication channel is indicated as MU $\leftarrow$ SU link – to an emitted signal by the master unit towards the slave unit – also indicated as MU $\rightarrow$ SU signal, while a corresponding communication channel is indicated as MU $\rightarrow$ SU link in the following – originating at the MU.

Full-duplex technologies and systems are of great interest because they will enable many 6G services, and the potential applications and challenges are discussed in [24]. Furthermore, in any radar system, the sensing capability is guaranteed by a full-duplex system that sends a signal and captures the signal back. Moreover, any combination of communication for 6G and sensing are based on full-duplexing, and this is another context of 6G. In the following exemplary study case, the MU $\rightarrow$ SU link uses a portion of the bandwidth Bd in the spectrum. The SU uses the STMM to back-reflect and modulate the received MU $\rightarrow$ SU signal with a phase-only MU $\leftarrow$ SU signal with a bandwidth Bu. The resulting full duplex signal, MU$\rightleftarrows$ SU signal in the following occupies a total bandwidth of B_{tot} = Bd + Bu, as detailed in the following. The SU relies solely on the STMM to encode the information, opening up to intriguing applications in severe energy-constrained scenarios. To summarize, the embodiments of the present invention are based on the following:

- A mathematical model for STMM-based wireless communication (MU SU).
- The SU terminal back reflects the signal adding information to the MU by time-modulating the phase of the STMM. Advantageously, a modulated feed signal at the STMM for MU $\leftarrow$ SU signal is used over back reflections.
- An analytical characterization of the coupling between the spatial and temporal phases in STMM, evaluating their practical impact on the proposed communication model.
- Two STMM implementations, one allowing the temporal phase to be changed at each element of the STMM and the other, cost-effective, that only requires a single time-varying phase shifter, common to all the elements. Space-time coupling strongly limits the reception angles, the size of the metasurface, and the MU $\leftarrow$ SU communication rate, giving rise to a cut-off to back-reflection MU $\leftarrow$ SU bandwidth limit.
- A method for space-time coupling compensation within the cut-off region, enabling a flexible and reliable implementation of the proposed communication model.
- An upper-bound performance assessment of the proposed model to form the guidelines for proper STMM design based on the main design parameters, i.e., transmitted power, MU-SU distance, and size of the metasurface.
- A maximum capacity achievable of the MU$\rightleftarrows$ SU signal considering the generic phase modulation for back-reflection, namely continuous phase modulation (CPM) with and without countermeasures for space-time coupling.

Notation: Bold upper- and lower-case letters describe matrices and column vectors, respectively. The (i, j)-th entry of matrix **A** is denoted by $[\mathbf{A}]_{(i,j)}$. Matrix transposition, conjugation, conjugate transposition and Frobenius norm are indicated respectively as $\mathbf{A}^T$, $\mathbf{A}^*$, $\mathbf{A}^H$ and $\|\mathbf{A}\|_F$. tr(**A**) extracts the trace of **A**. diag(**A**) denotes the extraction of the diagonal of **A**, while diag(**a**) is the diagonal matrix given by vector **a**. In is the identity matrix of size n. With **a** ~ CN (μ, C) we denote a multi-variate circularly complex Gaussian random variable a with mean μ and covariance C. **E**[·] is the expectation operator, while *R* and *C* stand for the set of real and complex numbers, respectively. δn is the Kronecker delta.

The embodiments of the invention comprise a wireless device and to a wireless network using the device. The invention also relates to a method for transmitting information data in a wireless network.

Figure 2 discloses a wireless network comprising three network nodes 1100, 1101, 1102. A network node is a device that is able to exchange information on the network, in particular to transmit and/or receive information.

In the non-limiting example of Figure 2, network node 1101 transmits an incident electromagnetic wave 1130 on a reflective surface 1110 of the network node 1100. The incident electromagnetic wave 1130 can be a wave carrying no information, e.g. a sinusoidal wave at a predetermined frequency f_0 that is known to node 1101. Alternatively, the incident electromagnetic wave 130 can be an electromagnetic wave carrying information, e.g. a frequency or amplitude modulated wave carrying information data.

The reflective surface 1110 comprises an array of reflective elements 1111 (also known as metasurface atoms) organized in matrix shape along two orthogonal directions x1 and y1. As an example, the array can be made of Mu = Mu,x x Mu,y elements, where Mu,x is the number of elements along the x1 direction, and Mu,y is the number of elements along the direction y1; in this case we can indicate each element of the array as (q,v), with q and v being to integers, such that q = 1, …, Mu,x and v = 1, …, Mu,y. As an example, each element of the array can be constituted by an antenna.

Preferably, the reflective surface 1110 is a metasurface of known type, comprising reflective elements 1111 having complex reflective coefficient that can be varied in phase or amplitude and phase by applying a suitable control signal to the reflective element.

The reflective elements have arbitrary dimensions, preferably each dimension of a reflective element is lower than the wavelength of the incident electromagnetic wave. The incident electromagnetic wave, therefore, can hit, and therefore be reflected by, a plurality of reflective elements, as illustrated in Figures 3a and 3b.

Node 1100 also comprises a control unit 1120 that is operatively connected to each reflective element 1111 in order to change their reflective coefficient, so as to change the propagation direction of the reflected electromagnetic wave 1140 and the informative content to be transmitted.

During a setting phase, the direction of the incident electromagnetic wave 1130 and of the reflected electromagnetic wave 1140 are determined, either automatically by node 1100, by the geometric configurations (i.e., corresponding or depending on reflective angles of the reflective elements) of 1100, 1101, 1102 – which can be fixed, changing due to the node moving in space – or by a manual input of an operator. Systems to align wireless nodes are known in the telecommunication field, e.g. to align radio bridges and can also be used in this case to align node 1100 with node 1101 and node 1102. Preferably, particularly in case of a node moving in space, the geometric configuration of the reflective elements is periodically evaluated by suitable means.

After the setting phase, the control unit 1120 is therefore aware of the incident angles θi, ϕi and the reflection angles θr, ϕr. The incident angles θi, ϕi is the angle formed between the direction of propagation of the incident electromagnetic wave 140 and a plane in which the reflective surface 1110 lays. The reflected angles θr, ϕr is the angle formed between the direction of propagation of the reflected electromagnetic wave 1140 and the plane in which the reflective surface 1110 lays.

Based on the incident angles θi, ϕi and the reflection angles θr, ϕr , the control unit 1120 determines, for each reflective element (q,v), a decoupling correction factor as follows

$$\Delta t_{q,v} = q d_x \frac{\cos\theta_i \cos\phi_i}{c} + q d_y \frac{\cos\theta_i \sin\phi_i}{c} \qquad \text{(f1)}$$

wherein

d_x is the distance between two consecutive reflective elements in the x1 direction, d_y is the distance between two consecutive reflective elements in the y1 direction, *c* is the speed of light.

This decoupling correction factor is then used by the control unit 1120 for a time-space modulation of the incident electromagnetic wave. By time- and space-modulating the incident electromagnetic wave, node 1100 is able to transmit further information to node 1102.

In particular, the control unit 1120 is configured for receiving an information signal $\gamma(t)$ and to add this information in the reflected electromagnetic wave. This is obtained by a modulating the time-dependent component of the phase of the reflected electromagnetic wave with the information signal Υ(t) and introducing the decoupling correction factor in the time-dependent component of the phase.

More in detail, the control unit 1120 is configured to control each reflective element 1111 so that the temporal phase of each reflective element is delayed compensating for the propagation delay caused by the wavefront.

In one embodiment (shown in Figure 3a) also indicated as architecture A in the following, each reflective element is associated to a space-time shifter of the reflective elements, adapted to introduce a phase delay $\beta_{q,v}(t)$ in the incident electromagnetic wave. For each reflective element, the control unit 1120 therefore modifies the phase of the incident electromagnetic wave by adding a phase delay; the phase delay of the (q,v)-th element being

$$\beta_{q,v}(t) = \varphi_{q,v} + \gamma\left(t + \Delta t_{q,v}\right) \quad \text{(f2)}$$

Wherein $\varphi_{q,v}$ is the space modulation component

$$\varphi_{q,v} = \frac{\pi}{2}\left(q\left(\cos\theta_i \cos\phi_i + \cos\theta_r \cos\phi_r\right) + v\left(\cos\theta_i \sin\phi_i + \cos\theta_r \sin\phi_r\right)\right) \quad \text{(f3)}$$

And $\gamma\left(t + \Delta t_{q,v}\right)$ is the time modulation component.

In one embodiment (shown in Figure 3b) also indicated as architecture B in the following, each reflective element is associated to a space phase shifter, while only one time phase shifter is used. In this case, the time-shifter introduces a time delay equal to $\gamma(t)$, while the space phase delay introduced by the space shifter is corrected by a factor decoupling correction factor multiplied for the derivative of the signal $\gamma(t)$. As a result, for each reflective element, the control unit 1120 therefore modifies the phase of the incident electromagnetic wave by adding a phase delay; the phase delay of the (q,v)-th element being

$$\beta_{q,v}(t) = \varphi_{q,v} + \gamma(t) - \gamma^{(1)}\left(\Delta t_{q,v}\right) \quad \text{(f4)}$$

Wherein $\gamma^{(1)}$ is the first order derivate of $\gamma(t)$.

In both configurations (Figures 3a and 3b), therefore the control unit modifies the phase of the incident electromagnetic wave by adding a phase shift which depends (i) on the information that the control units 1120 is requested to add, (ii) on the incident angles θi, ϕi and the reflection angles θr, ϕr , (iii) on the space distance between the reflective elements.

In one embodiment a mix of architecture A (disclosed in Figure 3a) and of architecture B (disclosed in Figure 3b) can be used. In this case there will be two groups of reflective elements: a first group being configured according to architecture A and a second one being configured according to architecture B (i.e. with one common time phase shifter). In this case the control unit will control each group of reflective elements as described above.

As shown in Figure 4, another embodiment or architecture C entails that the reflective surface 1110 is made of a plurality of blocks 1115, each block comprising a plurality of reflective elements 1111. Each block 1115 contains one time modulated shifter, thus presenting a lower complexity than architecture A. Different blocks can comprise a different number of reflective elements, or can comprise the same number of reflective elements. The time phase shifters of each plurality of blocks 1115 is preferably configured as disclosed above with respect to Architecture A, taking into account the relative delay introduced on each single element.

Further, each block 1115 comprises a space phase shifters. Thus, each block 1115 is configured as disclosed above with respect to architecture B.

In other words, architecture C can be regarded as a mixed architecture.

Thereby, assuming for simplicity that each block 115 has $M'_u = M'_{u,x} \times M'_{u,y}$ elements, such that the total number of elements is $M_u = L\, M'_{u,x} \times K\, M'_{u,y}$, with L and K, being the number of blocks along the direction x and y, the phase shift introduced by each element can be expressed as

$$\beta_{q,v}(t) = \varphi_{q,v} + \gamma\big(t + \Delta t^{i,j}_{q,v}\big) - \gamma^{(1)}\big(\Delta t^{i,j}_{q,v}\big) \qquad \text{(f5)}$$

$$\Delta t^{i,j}_{q,v} = [q + (i-1)M_{u,x}]\,\Delta t_x + [v + (j-1)M_{u,y}]\,\Delta t_y \qquad \text{(f6)}$$

For i=1,…, L, and j=1,…,K.

In one embodiment, the invention is directed to a device for use in a wireless network, which comprises a reflective surface and a control unit as described above for node 1100, and further comprises a source of electromagnetic waves, the source of electromagnetic waves being suitable for transmitting an electromagnetic wave on the reflective surface 1110. In this way, the source of electromagnetic waves behaves like node 1101 of Figure 2, sending an electromagnetic wave on the reflective surface.

The invention is also directed to a method for transmitting information in a wireless network. According to an embodiment of the invention the method comprises:

- determining the incident angle of an incident electromagnetic wave, the incident electromagnetic wave hitting a plurality of reflecting elements of a reflecting surface,
- determining the reflection angle of a reflected wave, the reflected electromagnetic wave being transmitted by the plurality of reflecting elements being hit by the incident electromagnetic wave,
- acquiring an information to be added to the incident electromagnetic wave, and
- controlling each reflecting element of the array in order to modify the phase of the incident electromagnetic wave by adding a phase shift which depends (i) on the information that the control units 120 is requested to add, (ii) on the incident angles θi, ϕi and the reflection angles θr, ϕr, (iii) on the space distance between the reflective elements or any constitutive elements arrangements.

As described above, the phase shift can be either

$$\beta_{q,v}(t) = \varphi_{q,v} + \gamma\big(t + \Delta t_{q,v}\big)$$

or

$$\beta_{q,v}(t) = \varphi_{q,v} + \gamma(t) - \gamma^{(1)}\big(\Delta t_{q,v}\big)$$

or

$\beta_{q,v}(t) = \varphi_{q,v} + \gamma\left(t + \Delta t_{q,v}^{i,j}\right) - \gamma^{(1)}\left(\Delta t_{q,v}^{i,j}\right)$

Depending on the different architecture of the device.

Although the invention has been disclosed with reference to a wireless device comprising a reflecting surface 1110, the invention is not limited to the above examples.

In alternative solutions, the wireless network is provided with a transmitting surface comprising a plurality of transmitting elements 211, as illustrated in Figure 5.

In Figure 5, a wireless network comprises a transmitting node 201 and a receiving node 202. Instead of transmitting directly to node 202, transmitting node 201 transmits an electromagnetic wave 230 to an intermediate node 200. The incident electromagnetic wave 230 impinges on the transmitting surface 210 of node 200. In the same way as described above for the other examples, the incident wave 230 can carry or not information.

In the same way of node 100 described above, also node 200 is provided with a control unit 220 that is operatively connected to the transmitting elements 211 to modify the transmitting coefficient of each transmitting elements, so as to control the direction and content of the electromagnetic wave 240 that is transmitted to node 202. In other words, control unit 220 controls the transmitting elements 211 to obtain a space-time modulation of the incident electromagnetic wave 230.

During a set-up phase, the direction of the incident electromagnetic wave 230 and of the transmitted electromagnetic wave 240 are determined. Based on this information, on the distance of the transmitting elements, and on the information γ(t) that has to be added to the incident electromagnetic wave, the control unit determines the space-time phase shift $\beta_{q,v}(t)$ that has to be introduced by each transmitting element being impinged by the incident electromagnetic wave.

As for node 100, also in case of node 200 (using transmitting elements in place of reflective elements), the space-time phase shift $\beta_{q,v}(t)$ that is introduced by each transmitting element takes into account a decoupling correction factor that depends on the distance between two consecutive transmitting elements and the incident angles θi and ϕi. The decoupling factor can be written similarly to the case of reflection, as

$$\Delta t_{q,v} = q d_x \frac{\cos\theta_i \cos\phi_i}{c} + q d_y \frac{\cos\theta_i \sin\phi_i}{c}$$

and the phase shift for the (q,v)-th element of the transmitting array 210 is $\beta_{q,v}(t)$ that will be calculated according to formulas (f2), (f4) or (f5) depending on the architecture of the transmitting array, e.g. architecture A, B or C.

The invention is also directed to a method for transmitting information in a wireless network. According to an embodiment of the invention the method comprises:

- determining the incident angle of an incident electromagnetic wave, the incident electromagnetic wave hitting a plurality of transmitting elements of a transmitting surface,

- determining the transmission angle of a transmitted wave, the transmitted electromagnetic wave being transmitted by the plurality of transmitting elements being hit by the incident electromagnetic wave,
- acquiring an information to be added to the incident electromagnetic wave, and
- controlling each transmitting elements of the array in order to modify the phase of the incident electromagnetic wave by adding a phase shift which depends (i) on the information that the control units 120 is requested to add, (ii) on the incident angles θi, ϕi and the transmission angles θt, ϕt, (iii) on the space distance between the transmitting elements.

As described above, the phase shift for the *(q,v)*-th element of the transmitting array 210 is a $\beta_{q,v}(t)$ that will be calculated according to formulas (f2), (f4) or (f5) depending on the architecture of the transmitting array, e.g. Architecture A, B or C and considering in these formulas a decoupling correction factor

$$\Delta t_{q,v} = qd_x \frac{\cos\theta_i \cos\phi_i}{c} + qd_y \frac{\cos\theta_i \sin\phi_i}{c}.$$

Independently from the use of a node 100 with a reflective surface or of a node 200 with a transmitting surface, in some embodiments the control unit of the node (1120 or 220 in the above described examples) can be configured also to add an amplitude modulation of the reflected/transmitted wave.

However, it is clear that the above examples must not be interpreted in a limiting sense and the invention thus conceived is susceptible of numerous modifications and variations.

For example, although the invention has been disclosed with reference to a wireless system comprising a reflecting (transmitting) surface 1110 (210) where the incidence angles θi, ϕi and the reflection (transmission) angles θr, ϕr (θt, ϕt) describe a decoupling correction factor $\Delta t_{q,v}$ between the reflective (transmitting) elements, the invention is not limited to the above examples.

In alternative embodiments of the present invention (not described in detail), the wireless network is provided with a reflective (transmitting) surface comprising a plurality of reflective (transmitting) elements 211, where the decoupling correction factor $\Delta t_{q,v}$ can be obtained as the propagation delay of the electromagnetic wave (1130, 230) propagating between the transmitting node 1101 (201) and the *(q,v)*-th reflective (transmitting) element.

In further embodiments according to the present invention (not illustrated), a network node comprises a source of signals or, more generally, of electromagnetic emissions and reflective elements featuring a metasurface. In this case the signals source is aimed at the reflective elements of the very same network node.

As should be clear to the skilled person, an incident wave could be generated by any source, even an unknown source – *i.e.*, the incident wave could be accidentally hitting the reflective elements, or the network node could be adapted to exploit incident waves generated by “captured” one or more sources of opportunity. In other words, the wave emitted by the opportunity source needs not to be modulated but can be a continuous wave.

ANOMALOUS NONRECIPROCAL METASURFACE

The fundamental equations describing the behavior of an STMM are set forth below. The universal Snell’s law is a generalization when dealing with both spatial and temporal phase gradients across a metasurface. Let us consider the scheme depicted in Figure. 6, where a plane EM wave E_i is impinging on a 2D planar metasurface deployed on the xy plane. The incident wave can be expressed as

$$\mathbf{E}_i(\mathbf{x}, t) = \mathbf{a}_i\, e^{j\Psi_i(\mathbf{x},t)}, \tag{1}$$

where ai is the amplitude of the wave, whereas phase $\Psi_i(x, t)$ is fast varying in space and time.

Quantities

$$\frac{1}{2\pi}\frac{\partial \Psi_i(\mathbf{x}, t)}{\partial t} = f_i \tag{2}$$

$$\nabla_{\mathbf{x}}\Psi_i(\mathbf{x}, t) = \mathbf{k}_i, \tag{3}$$

are, respectively, the frequency f_i and the wavevector k_i of the incident wave. Let us define the reflection coefficient of the metasurface as

$$\Gamma(\mathbf{x}, t) = \alpha(\mathbf{x}, t)\, e^{j\beta(\mathbf{x},t)}, \tag{4}$$

where $a(x, t)$ and $\beta(x, t)$ denote the time- and space-varying amplitude and phase of the reflection coefficient of the STMM, respectively. Herein, the metasurface is a phase-only device, thus $\alpha(x, t) = \alpha \neq 0$ on the metasurface area. Similarly to (1), the reflected wave can be generally expressed as

$$\mathbf{E}_o(\mathbf{x}, t) = \mathbf{a}_o\, e^{j\Psi_o(\mathbf{x},t)}, \tag{5}$$

with $a_o \approx a_i$ under the assumption of ideal reflection, i.e., $\alpha = 1 \forall x, t$. The reflected wave is characterized by wavevector ko and frequency f_o, that follow from the universal Snell’s law as described in [14]:

$$\mathbf{k}_o - \mathbf{k}_i = \left[\frac{\partial\beta(\mathbf{x}, t)}{\partial x}, \frac{\partial\beta(\mathbf{x}, t)}{\partial y}, 0\right]^{\mathrm{T}}, \tag{6}$$

$$f_o - f_i = \frac{1}{2\pi}\frac{\partial\beta(\mathbf{x},t)}{\partial t}. \tag{7}$$

As it can be observed in (7), any spatial variation of the phase $\beta(x, t)$ produces a variation of the instantaneous wavevector ko, and a time variation of the phase $\beta(x, t)$ induces a variation of the instantaneous frequency f_o in the reflected wave. The design of $\beta(x, t)$ to control both direction (k_o) and frequency (f_o) of the reflected wave is discussed below with respect to temporal modulation.

SYSTEM AND CHANNEL MODEL

Let us consider the reference scenario depicted in Figure 7a and 7b, where a generic MU establishes a full-duplex link with a SU. To simplify, the MU is equipped with two uncoupled antenna arrays of N elements each, to enable full-duplex capabilities at MU. The SU is equipped with a planar STMM of $M_u = M_{u,x} \times M_{u,y}$ elements (along x and y respectively), and an Rx antenna array of Md elements. We assume that the STMM and the Rx array are co-located at the SU. The assumption concerning the SU is meant to conceptually separate for simplicity the device that receives MU → SU data from the MU ← SU data stream via back-reflection. Note that, it is possible to make a single device capable of both receiving and transmitting at the same time, for example, by connecting some elements of the metasurface to one (or more) RF chain as disclosed in R. Schroeder, J. He, and M. Juntti, "Passive ris vs. hybrid ris: A comparative study on channel estimation," in 2021 IEEE 93rd Vehicular Technology Conference (VTC2021-Spring), 2021, pp. 1–7.

In this case, the analytical derivations would be slightly different, but the results are equivalent to those investigated herein.

A. Signal model

The time-continuous signal from the MU can be generally expressed as

$$\mathbf{x}(t) = \mathbf{f}_d \, s_d(t) \tag{8}$$

where $\mathrm{f}_d \in \mathbb{C}^{N\times 1}$ is the spatial precoding vector and $s_d(t)$ is the MU → SU time-continuous information signal with bandwidth B_d, centered around the carrier frequency f_i. The MU → SU signal propagates over a high-frequency channel as described in T. S. Rappaport, Y. Xing, O. Kanhere, S. Ju, A. Madanayake, S. Mandal, A. Alkhateeb, and G. C. Trichopoulos, "Wireless communications and applications above 100 ghz: Opportunities and challenges for 6g and beyond," IEEE access, vol. 7, pp. 78 729–78 757, 2019, yielding a received signal at the SU:

$$
\begin{aligned}
y_d(t) &= \frac{1}{\sqrt{\varrho_d}}\mathbf{w}_d^H\mathbf{H}_d(t) * \mathbf{x}(t) + \mathbf{w}_d^H\mathbf{n}(t) = \\
&= \frac{1}{\sqrt{\varrho_d}}\mathbf{w}_d^H\mathbf{H}_d\mathbf{x}(t-\tau) + \mathbf{w}_d^H\mathbf{n}(t)
\end{aligned}
\tag{9}
$$

where ϱ_d represents the MU → SU path loss in power, * is the matrix convolution, $\mathrm{w}_d \in \mathbb{C}^{N\times 1}$ is the SU combiner, $\mathrm{H}_d(t) = \mathrm{H}_d\delta(t-\tau) \in \mathbb{C}^{M_d\times N}$ is the MU → SU MIMO channel matrix, composed of a spatial part, such that $\mathrm{E}[\|\mathrm{H}_d\|_\mathrm{F}^2] = NM_d$ E and a temporal part (consisting of the propagation delay by $\tau = D/c$, with c being the speed of light), while $\mathbf{n}(t) \sim \mathcal{CN}(\mathbf{0}, \sigma_n^2\mathbf{I}_{M_d}\delta(t))$ is the additive noise, spatially and temporally uncorrelated.

The Rx signal model at the MU can be evaluated by considering the propagation towards the STMM and its back-reflection to the MU. The MU → SU signal at the STMM is

$$
\mathbf{r}(t) = \mathbf{H}_i(t) * \mathbf{x}(t) \tag{10}
$$

where $\mathrm{H}_i(t) = \mathrm{H}_i\delta(t-\tau) \in \mathbb{C}^{M_u\times N}$ is the *forward* MIMO channel between the MU and the STMM. The signal r(t) undergoes the STMM phase reflection and then the convolution with the backward (MU ← SU) MIMO channel $\mathrm{H}_o(t) = \mathrm{H}_o\delta(t-\tau) \in \mathbb{C}^{N\times M_u}$, obtaining

$$
\begin{aligned}
y_u(t) &= \frac{1}{\sqrt{\varrho_u}}\mathbf{w}_u^H\mathbf{H}_o(t) * \mathbf{\Phi}(t)\mathbf{r}(t) + \mathbf{w}_u^H\mathbf{z}(t) = \\
&= \frac{1}{\sqrt{\varrho_u}}\mathbf{w}_u^H\mathbf{H}_o(t) * \mathbf{\Phi}(t)\left(\mathbf{H}_i(t) * \mathbf{x}(t)\right) + \mathbf{w}_u^H\mathbf{z}(t) = \\
&= \frac{1}{\sqrt{\varrho_u}}\mathbf{w}_u^H\underbrace{\mathbf{H}_o\mathbf{\Phi}(t-\tau)\mathbf{H}_i}_{\mathbf{H}_u(t)}\mathbf{x}(t-2\tau) + \mathbf{w}_u^H\mathbf{z}(t)
\end{aligned}
\tag{11}
$$

where ϱ_u is the UL path loss in power, $\mathrm{w}_u \in \mathbb{C}^{N\times 1}$ is the uplink combiner at the MU, z(t) $\sim \mathcal{CN}(\mathbf{0}, \sigma_z^2\mathbf{I}_N\delta(t))$litive noise at the MU array and $\mathbf{\Phi}(t) \in \mathbb{C}^{M_u\times M_u}$ denotes the time-varying STMM phase pattern matrix

$$
\mathbf{\Phi}(t) = \mathrm{diag}\left(\left[e^{j\beta_0(t)}, \cdots, e^{j\beta_{M_u-1}(t)}\right]\right). \tag{12}
$$

The time-varying phase is, in turn, discretized in space across the STMM elements. In (11), $\mathbf{H}_u \in \mathbb{C}^{N\times N}$ denotes the chain channel MU⇄ SU channel. Notice that, although $\mathbf{H}_u(t)$ is a time-varying function, the relation with x(t) is multiplicative, because the time-varying signal injected by the STMM $\Gamma(x,t)=e^{j\beta(x,t)}$ is the reflection coefficient. The UL channel is normalized such that $\mathrm{E}[\|\mathbf{H}_i\|_\mathrm{F}^2] = \mathrm{E}[\|\mathbf{H}_o\|_\mathrm{F}^2] = NM_u$ and as detailed in the following, it is $\mathrm{E}[\|\mathbf{H}_u(t)\|_\mathrm{F}^2] \leq N^2M_u^2$.

It should be noted that recoding and combining vectors, i.e., f_d and (w_d, w_u), are herein based on the perfect knowledge of channels $\mathbf{H}_d$(t) and $\mathbf{H}_u$(t) at both MU and SU side. Further, channel estimation at the SU can be obtained through conventional approaches and shared with the MU through feedback as described in M. Mizmizi, D. Tagliaferri, D.

Badini, C. Mazzucco, and U. Spagnolini, "Channel estimation for 6g v2x hybrid systems using multi-vehicular learning," IEEE Access, vol. 9, pp. 95 775–95 790, 2021.

in addition, the decoding of the MU ← SU information signal encoded in β(t) is possible thanks to the knowledge of the MU → SU one $s_d(t)$, that shall be removed by the MU to decode β(t).

B. Channel Model

The cluster-based multipath channel model is widely used in the design of mmWave and sub-THz wireless communication systems because it effectively captures the unique propagation characteristics of these frequencies as disclosed in A. Meijerink and A. F. Molisch, "On the physical interpretation of the saleh–valenzuela model and the definition of its power delay profiles," IEEE Transactions on Antennas and Propagation, vol. 62, no. 9, pp. 4780–4793, 2014. Since this document is framed for these frequencies, this model is used here. Any of the channel impulse responses in (9)-(11) can be written as

$$\mathbf{H}(t) = \sum_{p=1}^{P} \xi_p \, \mathbf{a}_N(\phi_p^t, \theta_p^t)\mathbf{a}_M^{\mathrm{H}}(\phi_p^r, \theta_p^r)\delta\left(t - \tau_p\right) \tag{13}$$

where *(i)* P is the number of paths, *(ii)* $\xi_p \sim \mathcal{CN}\left(0, \sigma_p^2\right)$ is the scattering amplitude of p-th path, such that $\sum_{p=1}^{P} \sigma_p^2 = 1$, *(iii)* τ_p is the propagation delay of the p-th path, *(iv)* $\mathrm{a}_L(\theta, \varphi)$ is the steering vector of either Tx or Rx, function of Tx and Rx angles, respectively $\left(\phi_p^t, \theta_p^t\right)$ and $\left(\phi_p^r, \theta_p^r\right)$, and normalized such that $\|\mathrm{a}_L(\theta, \varphi)\|_F^2 = L$. As common for communication systems operating through back-scattering, the two-way channel to/from the STMM is characterized by a single dominant path, as for radar systems described in M. Manzoni, D. Tagliaferri, M. Rizzi, S. Tebaldini, A. V. Monti-Guarnieri, C. M. Prati, M. Nicoli, I. Russo, S. Duque, C. Mazzucco, and U. Spagnolini, "Motion estimation and compensation in automotive mimo sar," 2022. Multiple bounces can be considered, but their path loss is orders of magnitude higher, and thus are here neglected, considering $P = 1$ for both forward $\mathbf{H}_i(t)$ and backward $\mathbf{H}_o(t)$ channels. The inter-element spacing of Tx and Rx arrays (at both MU and SU) is $\lambda_i/2$, while at STMM is $\lambda_i/4$, with $\lambda_i = c/f_i$ being the incident wavelength.

The steering vector at the STMM is

$$\mathbf{a}_{M_u}(\theta, \varphi) = \left[e^{-j\frac{\pi}{2}(q\cos\theta\cos\phi + v\cos\theta\sin\phi)}\right] \tag{14}$$

for $q = 0, \ldots, M_{u,x} - 1$, $v = 0, \ldots, M_{u,y} - 1$, where (θ, ϕ) can be either incident or reflection angles. The propagation path losses in power, ϱ_d and ϱ_u in (9)-(11) are modeled as

$$\varrho_d = \frac{2^4 \pi D^2}{\lambda_i^2}, \qquad \varrho_u = \frac{2^{12} \pi D^4}{\lambda_i^4} \tag{15}$$

where D is the MU/SU distance. The model in (15) is obtained by assuming that the effective area of the MU/SU arrays is equal to the physical one, which is approximated as $N(\lambda_i/2)^2$, and that the back-reflected cross-section of the STMM is equal to the one of a perfect metallic plate with an area of $M_u(\lambda_i/4)^2$ as if it is oriented towards the MU as disclosed in S. Ellingson, "Path loss in reconfigurable intelligent surface-enabled channels," in 2021 IEEE 32nd Annual International Symposium on Personal, Indoor and Mobile Radio Communications (PIMRC), 2021, pp. 829–835.

It should be noted that the MU ← SU path loss ϱ_u is here assumed as only dependent on the wavelength of the incident signal λ_i. As detailed below with respect to temporal modulation, this is true for STMM phases β(t) considered as stochastic, whose average time derivative is zero, i.e., $\mathbb{E}[\mathrm{d}\beta_m(t)/\mathrm{d}t] = 0$, as common for information-bearing signals. Differently, for $d\beta_m(t)/dt \neq 0$, (e.g., a simple frequency shifting), the denominator of ϱ_u would be $\lambda_i^2\lambda_o^2$, with λ_o derived from (7).

Additionally, the aforementioned system and channel models imply that the bandwidth of the incident signal $s_d(t)$ (B_d), compared to the size of the STMM M_u, is such that the unwanted beam squinting from spatially wideband effects can be avoided as disclosed in B. Wang, F. Gao, S. Jin, H. Lin, and G. Y. Li, "Spatial- and frequency-wideband effects in millimeter-wave massive mimo systems," IEEE Transactions on Signal Processing, vol. 66, no. 13, pp. 3393–3406, 2018.

This narrowband behavior is herein adopted, adhering to the RIS literature [3]. However, a more detailed insight into this assumption is given below.

TEMPORAL MODULATION

The principles of temporal modulation at the STMM and its peculiarities are defined herein below.

For the implementation of the STMM, the architectures A and B according to the embodiments of the present invention described above with reference to Figures 3a and 3b. With respect to architecture, A, each element of the metasurface is modeled with a phase shifter capable of generating both spatial and temporal components, in compliance with (4) for $a(x, t) = 1$.

Conversely, with respect to architecture B, each element is modelled with a single spatial phase shifter and a temporal phase shifter common to all the elements. The difference between architectures A and B is mainly the reduced cost/complexity of the second, which comes at the price of a slightly reduced performance, as will be discussed in the following.

To ease the analytical interpretation while maintaining generality, we consider the MU to use precoding and combining vectors perfectly aligned with the SU. Thus, we have that f_d and w_u are given, e.g., estimated by conventional approaches, e.g. as disclosed in

M. Mizmizi, D. Tagliaferri, D. Badini, C. Mazzucco, and U. Spagnolini, "Channel estimation for 6g v2x hybrid systems using multi-vehicular learning," IEEE Access, vol. 9, pp. 95 775–95 790, 2021. The system model in (11) simplifies as:

$$y_u(t) = \frac{N^2}{\sqrt{\varrho_u}} h_u(t) s_d(t - 2\tau) + z(t), \tag{16}$$

where

$$h_u(t) = \mathbf{h}_o^{\mathrm{H}} \boldsymbol{\Phi}(t - \tau) \mathbf{h}_i, \tag{17}$$

is the MU ← SU channel, given the forward and backward spatial channels $h_i = \xi_i a M_u(\theta_i, \phi_i)$ and $h_o = \xi_o\, a M_u(\theta_o, \phi_o)$ respectively. In a full-duplex setting such as the one depicted in Fig. 3, we have that the incident and reflection angles coincide, $\theta = \theta_o = \theta_i$, $\phi = \phi_o = \phi_i$.

The embodiments of the invention are based on the following. Let us consider the phase (12) applied at the STMM elements (according to architecture B) as the superposition of a spatial and a temporal component, such that at the (q, v)-th element is

$$\beta_{q,v}(t) = \varphi_{q,v} + \gamma(t), \tag{18}$$

for $q = 0, \ldots, M_{u,x} - 1$, $v = 0, \ldots, M_{u,y} - 1$, where $\varphi_{q,v}$ is the space component of the phase used to design a complete back-reflection of the impinging signal and $\gamma(t)$ is an information-bearing phase signal applied at each STMM element, and common to all. Model (18), adopted in the current literature [20] or X. Fang, M. Li, D. Ding, F. Bilotti, and R. Chen, "Design of in-phase and quadrature two paths space-time-modulated metasurfaces," IEEE Transactions on Antennas and Propagation, vol. 70, no. 7, pp. 5563–5573, 2022, can also be considered valid for architecture A when only one data stream is generated at the SU, as considered in this document.

Expanding (16) with (18), we obtain the expression

$$\begin{aligned} y_u(t) &= \rho \sum_{q=0}^{M_{u,x}-1} \sum_{v=0}^{M_{u,y}-1} e^{-j(\pi(q\cos\theta\cos\phi + v\cos\theta\sin\phi) - \varphi_{q,v} - \gamma(t - \Delta t_{q,v} - \tau))} s_d(t - 2\Delta t_{q,v} - 2\tau) + z(t) \overset{(a)}{\approx} \\ &\overset{(a)}{\approx} \rho \sum_{q=0}^{M_{u,x}-1} \sum_{v=0}^{M_{u,y}-1} e^{-j(\pi(q\cos\theta\cos\phi + v\cos\theta\sin\phi) - \varphi_{q,v} - \gamma(t - \Delta t_{q,v} - \tau))} s_d(t - 2\tau) + z(t) \overset{(b)}{\approx} \\ &\overset{(b)}{\approx} \rho \sum_{q=0}^{M_{u,x}-1} \sum_{v=0}^{M_{u,y}-1} e^{-j(\pi(q\cos\theta\cos\phi + v\cos\theta\sin\phi) - \varphi_{q,v})} e^{j\gamma(t-\tau)} s_d(t - 2\tau) + z(t) \end{aligned} \tag{19}$$

where $\rho = \xi_i \xi_o / \sqrt{\varrho_u}$ accounts for geometrical energy losses, while

$$\Delta t_{q,v} = \left(\frac{\lambda_i}{2\pi}\right) \frac{\mathbf{k}_i^T \mathbf{p}_{q,v}}{c} = q\Delta t_x + v\Delta t_y \tag{20}$$

is the additional propagation delay for the (q, v)-th STMM element, located in $\mathrm{p}_{q,v} = (\lambda_i/4)[q, v, 0]^T$, and

$$\Delta t_x = \frac{\lambda_i}{4}\frac{\cos\theta\cos\phi}{c}, \quad \Delta t_y = \frac{\lambda_i}{4}\frac{\cos\theta\sin\phi}{c} \tag{21}$$

are the propagation delays of the wavefront across two adjacent STMM elements displaced by $\lambda_i/4$ along x and y. In (19), the first term is the complete expression of the Rx signal for MU $\rightarrow$ SU $s_d(t)$ and MU $\leftarrow$ SU $\gamma(t)$ signals. Approximation (a) implies that there are no spatially wideband effects due to the MU $\rightarrow$ SU signal, namely $s_d(t - 2\Delta T) \approx s_d(t)$, where $\Delta T = M_{u,x}\Delta t_x + M_{u,y}\Delta t_y$ is the maximum delay across the STMM elements. Similarly, approximation (b) subtends that the MU $\leftarrow$ SU phase-only signal does not suffer the relative propagation delay across the STMM, thus $\gamma(t - \Delta T) \approx \gamma(t)$. Notice that approximation (b) in (19) has the further implication that the spatial phase component $\varphi_{q,v}$ is not affected by the temporal one $\gamma(t)$, i.e., they can be separated as assumed in [20] and, consequently, the reflection gain is maximized by a phase-only pattern (not a function of time) across the STMM

$$\varphi_{q,v} = \pi(q\cos\theta\cos\phi + v\cos\theta\sin\phi), \tag{22}$$

obtaining

$$y_u(t) \approx \rho\, N\, M_u\, s_u(t-\tau)\, s_d(t-2\tau) + z(t), \tag{23}$$

where $s_u(t - \tau) = e^{j\gamma(t-\tau)}$ denotes the MU $\leftarrow$ SU signal injected by the STMM modulating the MU signal $s_d(t - 2\tau)$ in a multiplicative way.

Notice that the approximation (a) holds whenever

$$2\Delta T << T_d, \tag{24}$$

where $T_d = 1/B_d$ is the symbol period of the MU $\rightarrow$ SU information signal $s_d(t)$, while approximation (b) holds for

$$\Delta T << T_u, \tag{25}$$

where T_u is the symbol period of the MU $\leftarrow$ SU phase signal $\gamma(t)$.

In general, neither approximation (a) nor approximation (b) hold for large-bandwidth systems and/or comparatively large STMM. Noteworthy, while the beam squinting due to $s_d(t)$ cannot be compensated (except by reducing the MU $\rightarrow$ SU bandwidth B_d), the coupling between spatial and temporal phase patterns applied to the STMM is peculiar to these wireless communication systems and its detrimental effects can be reduced. Therefore, it is possible to neglect the wideband effects due to $s_d(t)$, analyzing the space-time phase coupling herein below and proposing countermeasure for wideband MU $\leftarrow$ SU system further below.

A. Space-Time Phase Coupling

The space-time phase coupling of the STMM elements according to the embodiments of the present invention can be readily explained considering Figures 3a and 3b. A plane wave impinging on the (u, v)-th element of the STMM with angle (θ, ϕ), as depicted in Figures 3a and 3b, will be reflected back with the following phase:

$$\widetilde{\beta}_{q,v}(t) = \varphi_{q,v} + \gamma(t - \Delta t_{q,v}), \tag{26}$$

thus the phase $\gamma(t)$ experiences an element-specific time delay that depends on the incidence angles (θ, ϕ), which induces a spurious, and undesired, spatial phase gradient. This phenomenon leads to an unwanted decrease in the reflection gain. In other words, assuming the conventional spatial phase gradient detailed in (22), we have that the following theorem holds:

Theorem 1. Let hu(t) be the channel defined as in (17) and let the phase be defined as (18), with $\varphi_{q,v} = \pi(q \cos\theta \cos\phi + v \cos\theta \sin\phi)$, $u = 0, \ldots, M_{u,x} - 1$, $v = 0, \ldots, M_{u,y} - 1$. Then, it is:

$$\mathbb{E}_\gamma\left[|h_u(t)|^2\right] \leq M_u^2. \tag{27}$$

Proof. The proof can be readily carried out by inspection of the structure of $h_u(t)$, which yields

$$\mathbb{E}_\gamma\left[\left|\sum_{q=0}^{M_{u,x}-1}\sum_{v=0}^{M_{u,y}-1} e^{j\gamma(t-\Delta t_{q,v}-\tau)}\right|^2\right] \leq M_u^2. \tag{28}$$

To have equality in (28), the arguments of the complex exponential shall neither be a function of q nor of v (spatial and temporal phase decoupling). Therefore, the sufficient conditions are $\gamma(t) = \gamma$ (straightforward condition) or $\Delta t_x = \Delta t_y = 0$ $(\theta = \pi/2)$.

Theorem 1 implies that any phase-encoded modulation signal $\gamma(t)$ leads to a strict inequality for (28), except for very low MU $\leftarrow$ SU signal bandwidth, fulfilling (25), or the case in which the impinging wave is perfectly orthogonal to the STMM plane, i.e., $\theta = \pi/2$. To evaluate the space-time phase coupling effect, let us consider a generic non-linear $\gamma(t) : [a, b] \rightarrow \mathbb{R}$, infinitely differentiable for $t_0 \in (a, b)$. We can use the Taylor expansion around $t = t_0$, truncated at the n-th term

$$\gamma(t_0 - \Delta t_{q,v}) \approx \gamma(t_0) + \sum_{i=1}^{n-1} \frac{(\Delta t_{q,v})^i}{i!}\gamma^{(i)}(t_0). \tag{29}$$

where $\gamma^{(i)}(t_0)$ denotes the i-th time derivative of $\gamma(t)$ evaluated in $t=t_0$. Considering only the first order ($n = 1$) derivative only, namely

$$\gamma(t_0 - \Delta t_{q,v}) \approx \gamma(t_0) + \gamma^{(1)}(t_0)\Delta t_{q,v} \tag{30}$$

it is apparent that the second term is a linear phase shift with the element index that results in the so-called beam squinting, i.e., the angular shift of the reflected beam w.r.t. to the desired direction (θ, ϕ). This effect causes a reduction of the reflection gain that can be analytically evaluated from the STMM's array factor that adds up to a possible beam squinting due to a large-bandwidth $s_d(t)$ (herein not considered).

To quantify the beam squinting due to (30), let us consider a linear temporal phase signal (or piecewise linear, e.g., obtained with frequency shift keying (FSK) modulation) $\gamma(t) = 2\pi f_s t$, where $f_s = f_i - f_o$ is the frequency shift determined by the temporal component of the phase $\beta(x, t)$ as in (7). Let us express the frequency shift as $f_s = \kappa f_i$, where $\kappa \in \mathbb{R}$ is a coefficient that describes the frequency up- or down-conversion, or equivalently $f_o = f_i (1 + \kappa)$. By substituting the expression of $\gamma(t)$ in (28) and removing the expectation, we obtain

$$AF(\theta, \phi, \kappa) = \frac{1}{M_u} \sum_{q=0}^{M_{u,x}-1} \sum_{v=0}^{M_{u,y}-1} e^{j2\pi f_i \kappa (t - \Delta t_{q,v})}, \tag{31}$$

with the corresponding normalized reflection gain

$$|AF(\theta, \phi, \kappa)|^2 = \left| \frac{1}{M_u} \frac{\sin((\pi/4) M_{u,x} \kappa \cos\theta \cos\phi)}{\sin((\pi/4)\kappa \cos\theta \cos\phi)} \frac{\sin((\pi/4) M_{u,y} \kappa \cos\theta \sin\phi)}{\sin((\pi/4)\kappa \cos\theta \sin\phi)} \right|^2. \tag{32}$$

Considering for instance a 1D case (i.e., either a 1D STMM or $\phi = 0$), replacing $\Delta t_{q,v}$ in (20) with Δt_x in (21) ($\phi = 0$), the normalized reflection gain simplifies as

$$|AF_{1D}(\theta, \kappa)|^2 = \left| \frac{1}{M_u} \frac{\sin((\pi/2) M_u \kappa \cos\theta)}{\sin((\pi/2)\kappa \cos\theta)} \right|^2. \tag{33}$$

This allows gaining insight on the effective reflection gain of the STMM. Figure 8 depicts the impact of the space-time phase coupling on the normalized reflection gain, and for $\theta \neq \pi/2$ and $k \neq 0$, the system experiences a diminished reflection gain. For instance, at $\theta = \pi/6$ we observe a loss ≥ 3 dB ($M_u = 100 \times 100$) and ≥ 10 dB ($M_u = 200 \times 200$) for $\kappa > 2$ % (e.g., for a frequency shift of $f_s > 0.6$ GHz around $f_i = 30$ GHz). The loss w.r.t. the maximum reflection gain can be justified by the tilting of the direction of maximum reflection, that can be evaluated as

$$\tilde{\theta}_o = \arccos\left[(1 + \kappa)\cos\theta_o\right] \tag{34}$$

where $\widetilde{\theta_o}$ is the angle of maximum reflection, different from the true one $\theta_o = \theta_i$ due to the space-time phase gradient coupling. The trend of $\widetilde{\theta_o}$ with the frequency shift κ is shown in Figure 9. The result in (34) is obtained by substituting (30) and (22) in (19). Note that for $|\cos\theta(1 + \kappa)| > 1$ in (34) we have evanescent waves, as depicted in Figure 10.

Whenever the phase $\gamma(t)$ is periodic, or cyclo-stationary, the aforementioned approaches are specialized to the harmonics of the Fourier series decomposition of $\gamma(t)$ as experimentally observed in [17], [18]. To implement a wireless communication system using STMM technology, the spatial phase must be decoupled from the temporal one, such that the former can be used to back-reflect the impinging signal toward the MU and the latter to convey information.

B. Space-Time Phase Decoupling

Decoupling the spatial phase from the temporal phase can be achieved differently depending on the specific STMM architecture according to the present invention.

1) Architecture A: Decoupling can be achieved by delaying the temporal phase of each element to compensate for the propagation delay caused by the wavefront. Specifically, the phase of the *(q, v)*-th element must be set as:

$$\beta_{q,v}(t) = \varphi_{q,v} + \gamma(t + \Delta t_{q,v}). \tag{35}$$

To achieve perfect decoupling, assumed herein, the STMM phase shifters must be accurately time-synchronized using the knwoledge of the incident angles as input, e.g., after a proper estimation.

2) Architecture B: A straightforward yet effective countermeasure to space-time phase coupling is to pre-compensate the spatial phase by considering the induced effect of the temporal phase. In particular, the phase of the *(u, v)*-th element is

$$\beta_{q,v}(t) = \varphi_{q,v} + \gamma(t) - \gamma^{(1)}(t)\Delta t_{q,v}. \tag{36}$$

where the spatial phase $\varphi_{q,v}$ now incorporates the element-dependent delay $\Delta t_{q,v}$. As demonstrated in Section VI, architecture B allows for a cost reduction (only one phase shifter is required to vary over time) compared to architecture A, at the price of performance reduction for large bandwidth UL signals. The design of $\gamma(t)$, the requirements, and the achievable performance of the proposed communication system are discussed herein below.

UPLINK (UL) SIGNAL DESIGN

A MU → SU signal $y_d(t)$ can be designed following conventional methods (e.g., linear modulation or orthogonal frequency division multiplexing). According to an embodiment of the invention, the phase shape $\gamma(t)$ for controlled back-reflection by the STMM is designed according to the following criteria.

A. Continuous Phase Modulation

Let us consider that γ(t) is a continuous phase modulated (CPM) signal for MU ← SU:

$$\gamma(t) = 2\pi h \sum_n z_n q(t - nT_u) \tag{37}$$

where h is the modulation index, $z_n \in \{2b - 1\}$, $b \in \{-(M/2), ..., (M/2) - 1\}$, is the n-th M-ary information symbol, T_u is the MU ← SU symbol duration, and $q(t)$ is the phase pulse with the following properties

$$q(t) = \begin{cases} 0 & t \leq 0 \\ \frac{1}{2} & t \geq LT_u \end{cases} \tag{38}$$

where L represents the modulation memory. The phase pulse is usually defined as

$$q(t) = \int_{-\infty}^{t} p(\tau) d\tau \tag{39}$$

with $p(t)$ being the pulse shaping filter (PSF). The reason behind choosing CPM is that it represents the most general phase modulation for $\gamma(t)$. Indeed, depending on the parameters set M, h, L, and $p(t)$, the CPM can degenerate in the other phase modulations, such as phase shift keying (PSK), frequency shift keying (FSK), minimum shift keying (MSK), and Gaussian MSK (GMSK) as described J. B. Anderson, T. Aulin, and C.-E. Sundberg, Digital phase modulation. Springer Science & Business Media, 2013. The same reference can be used as introductory on CPM.

B. Bandwidth Occupancy

The bandwidth occupied by the MU → SU received signal $y_d(t)$ in (9), assuming a frequency-flat channel, is the bandwidth of the transmitted signal $s_d(t)$, i.e., the support of the power spectral density (PSD) $P_d(f) = \mathbb{E}\left[|\mathcal{F}\{s_d(t)\}|^2\right]$ where $\mathcal{F}\{.\}$ denotes the Fourier Transform operator.

Under the same channel assumption, the bandwidth occupied by the MU ← SU signal $y_u(t)$ in (11), is the support of its PSD, defined as

$$\begin{aligned} P_u(f) &= \mathbb{E}\left[|\mathcal{F}\{s_d(t)s_u(t)\}|^2\right] = \\ &= \mathbb{E}\left[|\mathcal{F}\{s_d(t)\}|^2\right] * \mathbb{E}\left[|\mathcal{F}\{s_u(t)\}|^2\right], \end{aligned} \tag{40}$$

and thus, according to the properties of the convolution, the total bandwidth of the system is

$$B_{tot} = B_d + B_u \tag{41}$$

with Bu being the support of $\mathbb{E}\left[|\mathcal{F}\{s_u(t)\}|^2\right]$. Notice that the resulting spectrum Pu(f) is centered around the carrier frequency f_i. This follows from the fact that the information-bearing phase signal $\gamma(t)$ has a time-derivative that is

$$\gamma^{(1)}(t) = 2\pi h \sum_n z_n p(t - nT_u) \tag{42}$$

that is zero on the ensemble average, i.e., $\mathbb{E}[\gamma^{(1)}(t)] = 0$, thus the average net frequency shift is zero. For a generic CPM signal, the occupied bandwidth is infinite, but the 99% of the signal energy is within

$$B_u = \frac{h}{T_u}\sqrt{\frac{g(M^2-1)}{3L}} + \frac{g}{T_u L} = \frac{\epsilon}{T_u} \tag{43}$$

where ϵ is the time-bandwidth product of the specific CPM implementation. In (43), the term g depends on the PSF p(t) used, e.g., $g = 1$ for rectangular and g=1.5 for raised cosine, as described in C.-H. Kuo and K. M. Chugg, "On the bandwidth efficiency of cpm signals," in IEEE MILCOM 2004. Military Communications Conference, 2004., vol. 1. IEEE, 2004, pp. 218–224.

The bandwidth occupation is inversely proportional to the CPM memory L. For $M = 2$, $g = 1$ (rectangular PSF), the bandwidth is $B_u = (h\sqrt{L} + 1)/(LT_u)$.

It is worth underlining that the proposed communication system is full-duplex, as MU $\rightarrow$SU and MU $\leftarrow$ SU communications occur simultaneously on the same spectrum portion B_{tot}. However, the spectral efficiency is equivalent to an FDD system, with Bd for MU $\rightarrow$ SU and B_u for MU $\leftarrow$ SU, as detailed in the following.

C. Spectral Efficiency

The performance of the system according to the present invention can be assessed in terms of spectral efficiency (SE), considering both MU $\rightarrow$ SU and MU $\leftarrow$ SU links. In particular, the SE upper bound given by Shannon's unconstrained SE is:

$$\eta = \underbrace{(1-\mu)\log_2(1+\Upsilon_d)}_{\eta_d} + \underbrace{\mu\log_2(1+\Upsilon_u)}_{\eta_u} \tag{44}$$

where the first term (η_d) is the SE of the MU $\rightarrow$ SU and the second (η_u) is the SE of the MU $\leftarrow$ SU. In (44), $\mu = B_u/Btot$ is the fractional bandwidth occupied by the MU $\leftarrow$ SU, and $1 - \mu = B_d/B_{tot}$ the MU $\rightarrow$ SU counterpart, while Υ_d and Υ_u are the45 MU $\rightarrow$ SU and MU $\leftarrow$ SU signal-to-noise ratios (SNRs) at the decision variable.

The MU $\rightarrow$ SU SNR is

$$\Upsilon_d \leq \frac{\sigma_{s,d}^2 N M_d}{\varrho_d \sigma_z^2} \tag{45}$$

where the equality holds when perfect CSI is available and optimal precoding/combing is employed, which both provide the maximum MIMO gain, i.e., NM_d.

The MU $\leftarrow$ SU Rx signal undergoes a matched filtering over T_u with the Tx signal $s_d(t-2\tau)$, that is clearly known at MU. Assuming the delay τ is known, the SNR can be analytically evaluated as described in the following, depending on whether the STMM exhibits a wideband behavior w.r.t. $\gamma(t)$ or not. A suitable upper bound on the SNR is obtained by assuming that the wideband regime involves the same UL symbol, i.e., $\Delta T < T_u$, yielding

$$\Upsilon_u \leq \frac{\sigma_{s,d}^2 N^2 M_u^2}{\varrho_u \sigma_z^2} |AF(\theta, \phi, \kappa)|^2 T_u B_{tot} \tag{46}$$

where $|AF(\theta, \phi, \kappa)|^2 \leq 1$ is the loss due to the space-time phase coupling, defined in (32), and $T_u B_{tot}$ is the processing gain of the matched filter. The latter is motivated by the fact that, while the MU ← SU noise z(t) occupies the whole bandwidth B_{tot}, the signal only occupies a fraction of it μB_{tot}. Thus, the matched filter makes the MU ← SU SNR inversely proportional to the fractional bandwidth occupation, $\Upsilon_u \propto 1/\mu$. The equality in (46) holds under the following conditions: (i) perfect CSI available at both MU and SU, (ii) known delay τ at the MU, and (iii) constant phase $\gamma(t) \in [0, T_u)$.

The MU → SU and MU ← SU capacity in (44) has a global optimum with respect to the unconstrained UL bandwidth allocation μ. From the derivative of η w.r.t. μ

$$\frac{d\eta}{d\mu} = -\log_2(1+\Upsilon_d) - \frac{\widetilde{\Upsilon}_u \log_2 e}{\widetilde{\Upsilon}_u + \mu} + \log_2\left(1 + \frac{\widetilde{\Upsilon}_u}{\mu}\right) = 0 \quad (47)$$

whose root provides the optimal duplexing allocation. In (47), we denote with $\widetilde{\Upsilon}_u$ the MU ←SU SNR terms that do not depend on the allocation μ.

NUMERICAL RESULTS

Numerical and analytical results for the STMM-based wireless communication system according to the present invention are herein provided, aimed at gaining insight on upper achievable performance, operating conditions and possible limitations. In all the following, the frequency of operation is f_0 = 30 GHz. We consider a CPM modulation with a rectangular PSF, L = 1, and M-ary= 2, where $\kappa = h/(2\,T_u)$. This coincides with CP-FSK for h = 1 and an MSK for h = 1/2. The trends and considerations are the same for a generic CPM or any phase/frequency modulation, but the absolute values must be derived case by case.

The first set of results, summarized in Figures 11a, 11b and 11c, shows the achievable SE (both MU → SU and MU ← SU) utter performance varying system parameters. These results are based on (46) when $|AF(\theta, \phi, \kappa)|^2 = 1$, which can be attained for: *(i)* architecture A with space-time decoupling (35), *(ii)* architecture B with space-time decoupling (36) and limited bandwidth Bu, and *(iii)* normal incidence, i.e., θ_i = 90 deg. In all cases, we have μ = 0.5, thus the same bandwidth for MU → SU and MU ← SU. Figure 11a shows the SE varying the MU → SU equivalent single-input single-output SNR, namely

$$\Upsilon_0 = \frac{\Upsilon_d}{N M_d} = \frac{\sigma^2_{s,d}}{\varrho_d\, \sigma^2_z}, \quad (48)$$

as well as the number of MU antennas N and STMM elements Mu. The MU⇄ SU link length is fixed to D = 100 m and the number of SU Rx elements Md = 8×4. We notice the dramatic impact of the number of STMM elements Mu that allows boosting the MU ←

SU SE (up to be higher than the MU $\rightarrow$ SU one for Mu = 200×200). A similar effect, though to a lesser extent, is obtained by increasing N. The trend of the SE varying the MU$\rightleftarrows$ SU link length D is instead shown in Figure 11b. For fixed MU $\rightarrow$ SU performance η_d, the UL one rapidly decays with D, still being higher than the former one for massive MU arrays and STMM (i.e., a comparatively high number of STMM elements). As can be expected, when N is fixed, e.g., by technological limitations, the overall MU $\leftarrow$ SU SE η_u is mostly ruled by the number of STMM elements Mu, as confirmed by Figure 11c, where the SE is let vary as a function of the STMM size (side number of elements $\sqrt{M_u}$), for D = 50 m and D = 100 m. The results in Figures 11a-c show that with an appropriate design, the STMM can provide excellent MU $\leftarrow$ SU performance even at relatively large distances, comparable with the cell radius in current mmWave 5G systems. Remarkably, most of the energy employed to achieve η_d and η_u is spent at the MU, while the SU does not need a power amplifier. However, wideband effects due to the MU $\leftarrow$ SU signal γ(t) practically limit the performance and, mostly, the MU $\leftarrow$ SU bandwidth Bu, as discussed in the following.

The wideband effects on the STMM operation are shown in Figures 12a (for $M = 100 \times 100$) and 12b (for $M = 200 \times 200$), reporting the MU $\leftarrow$ SU SE η_u varying κ, i.e., the equivalent linear frequency shift due to the modulating signal $\gamma(t)$. We assume $Bu \gg Bd$, such that to ignore any wideband effect due to the MU $\rightarrow$ SU signal $s_d(t)$, that is the approximation (a) in (19). The distance is D = 100 m and $N = 32 \times 16$. The aim of these results is to quantitatively examine the impact of the space-time phase coupling at the STMM. The analysis in Section IV-A has shown that the space-time coupling is not influenced by transmitted power or distance, but rather by MU $\leftarrow$ SU bandwidth B_u, angle of incidence/reflection (θ, ϕ), and the size of the STMM Mu. Figures 12a and 12b consider both architectures A and B, with ideal compensations (35)-(36), respectively, and two incidence angles, θ = 30, 60 deg (ϕ = 0 deg for simplicity). The non-compensation case is shown as a benchmark.

Considering architecture B, where only one time-varying phase shifter is present (and common to all the STMM elements), the UL SE η_u progressively degrades for increasing grazing incidence angles ($\theta \rightarrow 0$ deg) and STMM elements Mu. In both Fig. 12a and 12b, it is possible to distinguish three operation regions, outlined in the following SNR analysis and corresponding to *(i)* $\Delta T \ll T_u$, i.e., ideal narrowband STMM operation; *(ii)* $\Delta T \leq T_u$, i.e., wideband STMM operation without ISI; *(iii)* $\Delta T > T_u$, i.e., wideband STMM operation with ISI. The first operation region occurs for very low modulation bandwidths (e.g., $\kappa \leq 1\%$ for $M_u = 100 \times 100$, θ = 30 deg and κ ≤ 0.5% for Mu = 200 × 200, θ = 30 deg), limiting the effective MU $\leftarrow$ SU throughput. The second operation region happens for larger modulation bandwidths, up to a cut-off frequency κ (e.g., κ ≤ κ = 1.9% for $M_u = 100 \times 100$, θ = 30 deg and κ ≤ κ = 1% for $M_u = 200 \times 200$, θ = 30 deg). In this regime, the STMM benefits from the space-time decoupling (36) to improve the SE η_u. Above the cut-off limit κ, the STMM realized with architecture B does not work properly: the SNR after the matched filter Y_u is abated by the presence of the ISI from past modulation symbols in $\gamma(t)$ (see SNR analysis). The performance rapidly drops to zero. However, we want to remark that past symbols represent ISI as far as the simple matched filter approach (before trellis decoding) is adopted. In principle, the Rx can be designed to account for the unwanted additional delay due to the STMM reflection; however, this would increase the complexity of the implementation and it is not considered here.

Concerning the optimal choice of μ, namely the bandwidth splitting between MU → SU and MU ← SU, it depends on the size of the STMM and the distance between the MU and SU.

Figure 13 shows the MU → SU, MU ← SU, and total SE η_d, η_u and η respectively, varying μ for D = 100 m, N = 32×16, and assuming ideal narrowband STMM behavior (upper-performance limit). The total SE shows a peak, as predicted by (47), that depends on the number of STMM elements M_u. This result can have two readings: one can maximize the spectral efficiency η over the entire bandwidth B_{tot}, and thus the fraction μ allocated depends on the specific setup, or one can allocate the fraction μ based on the MU and SU requirements, but the spectral efficiency η over the entire band may not be optimal. In other words, the method used to allocate the fraction μ of the band can be based on either maximizing overall spectral efficiency η or on specific MU and SU requirements. While maximizing overall spectral efficiency η is desirable in some cases, it may not be the best approach if the MU and SU requirements must be met. In such cases, one may have to compromise on the overall spectral efficiency η in order to meet the requirements of the MU and SU.

SNR ANALYSIS

The Rx signal at the MU side undergoes matched filtering and phase estimation, before being fed to the sequence detector, e.g., Viterbi. We derive the SNR after the matched filter at the MU in the assumption that the Rx signal is the one expressed by (19), approximation (a). The estimated phase at the n-th MU ← SU symbol is provided by

$$\hat{\gamma}(nT_u) = \arg\left\{ r_n = \int_{nT_u}^{(n+1)T_u} y_u(t) s_d^*(t-2\tau)dt \right\}. \tag{49}$$

The SNR is obtained from r_n with a double expectation over the Tx signal $s_d(t)$ and the modulating phase $\gamma(t)$. The power of the useful signal part is

$$\begin{aligned}\sigma^2_{signal} &= \mathbb{E}_{s,\gamma}\left[\left|\int_{T_u} \rho |s_d(t-2\tau)|^2 \sum_{u,v} e^{j\gamma(t-\Delta t_{u,v}-\tau)}\right|^2 dt\right] \leq \\ &\leq \mathbb{E}_s\left[\int_{T_u} |\rho|^2 |s_d(t-2\tau)|^4 dt\right] \mathbb{E}_\gamma\left[\int_{T_u}\left|\sum_{u,v} e^{j\gamma(t-\Delta t_{u,v}-\tau)}\right|^2 dt\right] \approx \\ &\approx |\rho|^2 \sigma^4_{s,d} T_u \, \mathbb{E}_\gamma\left[\int_{T_u}\left|\sum_{u,v} e^{j\gamma(t-\Delta t_{u,v}-\tau)}\right|^2 dt\right]\end{aligned} \tag{50}$$

where we made use of the Schwartz inequality and assume, for simplicity of exposition, that the MU $\rightarrow$ SU signal $s_d(t)$ has a constant power $\sigma^2_{s,d}$ within the integration interval T_u. According to the size of the STMM M_u=$M_{u,x}$×$M_{u,y}$ compared to the MU $\leftarrow$ SU bandwidth Bu (related to the symbol time through (43)), we can distinguish three cases, as detailed in the following.

1) $\Delta T \ll T_u$: In this case, the STMM exhibits a narrowband behavior w.r.t. to the MU $\leftarrow$ SU signal, namely the variation of γ(t) across the STMM can be neglected. Therefore, we have

$$\mathbb{E}_\gamma\left[\int_{T_u}\left|\sum_{u,v} e^{j\gamma(t-\Delta t_{u,v}-\tau)}\right|^2 dt\right] \approx M_u^2 T_u \tag{51}$$

and the reflection gain is maximized under the assumption of the perfect knowledge of the channel (i.e., perfect spatial phase configuration in (43)). The power of the noise after the matched filter is

$$\sigma^2_{noise} \leq N_0 \sigma^2_{s,d} T_u \tag{52}$$

(including the beamforming gain at the MU), thus the SNR is upper-bounded by

$$\Upsilon_u = \frac{\sigma^2_{signal}}{\sigma^2_{noise}} \leq \frac{|\rho|^2 M_u^2 \sigma^2_{s,d}}{\sigma^2_z} T_u B_{tot} \tag{53}$$

from which follows (46) by expanding ρ.

2) $\Delta T \leq T_u$: In this case, the STMM exhibits a wideband behavior w.r.t. to the MU$\leftarrow$ SU signal, namely the variation of γ(t) across the STMM cannot be ignored in (50), but it is less than the symbol duration. Now, we have

$$\mathbb{E}_\gamma\left[\int_{T_u}\left|\sum_{u,v} e^{j\gamma(t-\Delta t_{u,v}-\tau)}\right|^2 dt\right] \approx M_u^2 |AF(\theta,\phi,\kappa)|^2 T_u \tag{54}$$

it yields the case explored in Section IV with the beam squinting effect. The SNR upper bound

$$\Upsilon_u \leq \frac{|\rho|^2 M_u^2 \sigma_{s,d}^2}{\sigma_z^2} |AF(\theta,\phi,\kappa)|^2 T_u B_{tot}. \tag{55}$$

3) $\Delta T > T_u$: In this case, the STMM exhibits a wideband behavior w.r.t. to the MU← SU signal and the variation of γ(t) across the STMM exceeds the symbol duration. This means that the MU receives a signal with multiple superposed symbols, and the STMM elements can be clustered according to the specific MU←SU symbol they are reflecting at a given instant of time.

Considering for simplicity a linear STMM, we have $C = \lceil M_u \Delta t / T_u \rceil$ spanned symbols, where Δt is the propagation delay across two adjacent elements, Δt = (λi/4)(cos θ/c). Considering a 2D STMM again, we can define the following set of STMM elements:

$$\begin{aligned} \mathcal{M}'_u &= \{(u,v) | \Delta t_{u,v} < T_u\} \\ \mathcal{M}''_u &= \{(u,v) | \Delta t_{u,v} \geq T_u\} \end{aligned} \tag{56}$$

for u = 0, ...,$M_{u,x} - 1$, v = 0, ...,$M_{u,y} - 1$, where the first one indicates the symbol of interest and the second all the remaining $C - 1$ ones. Notice that estimating the phase with the simple matched filter in (49) implies that the $C - 1$ symbols other than the n-th of interest act as inter-symbol interference (ISI). Therefore, we have the following relation

$$\mathbb{E}_\gamma\left[\int_{T_u}\left|\sum_{u,v} e^{j\gamma(t-\Delta t_{u,v}-\tau)}\right|^2 dt\right] \approx \underbrace{|\mathcal{M}'_u|^2 |AF(\theta,\phi,\kappa)|^2 T_u}_{\text{useful signal}} + \underbrace{\mathbb{E}_\gamma\left[\int_{T_u}\left|\sum_{(u,v)\in\mathcal{M}''_u} e^{j\gamma(t-\Delta t_{u,v}-\tau)}\right|^2 dt\right]}_{\text{ISI}} \tag{57}$$

and thus the useful signal power is

$$\sigma_{signal}^2 \approx |\rho|^2 \sigma_{s,d}^4 |\mathcal{M}'_u|^2 |AF(\theta,\phi,\kappa)|^2 T_u^2 \tag{58}$$

while the ISI power σ_{ISI}^2comes from the integration across different symbols, with detrimental effects on system performance. The SNR turns into SINR as

$$\Upsilon_u = \frac{\sigma_{signal}^2}{\sigma_{ISI}^2 + \sigma_{noise}^2} = \frac{|\rho|^2 \sigma_{s,d}^4 |\mathcal{M}'_u|^2 |AF(\theta,\phi,\kappa)|^2 T_u^2}{\sigma_{ISI}^2 + N_0 \sigma_{s,d}^2 T_u}. \tag{59}$$

However, it is clear that the above examples must not be interpreted in a limiting sense and the invention thus conceived is susceptible of numerous modifications and variations.

Naturally, all the technical elements of devices and systems described above can be replaced with other technically-equivalent elements.

As will be evident to the person skilled in the art, one or more steps of methods described above can be carried out in parallel with each other or in a different order from the one presented above. Similarly, one or more optional steps can be added or removed from one or more of the procedures described above.

CLAIMS

1. A wireless communication device comprising:

- an array (1110) of reflective elements (1111) adapted to reflect an incident electromagnetic wave (1130), and
- a control unit (1120) operatively connected to each reflective element of the array in order to space-time modulating the incident electromagnetic wave to transmit additional information with the reflected electromagnetic wave (1140),

wherein the control unit is configured to control each reflective element in order to introduce, in the incident electromagnetic wave that hits the reflective element, a phase shift which depends (i) on the additional information to be transmitted, (ii) on the incident angles θ_i and ϕ_i formed between the plane on which the array rests and the incident electromagnetic wave, (iii) on the reflection angles θ_r and ϕ_r formed between the plane on which the array rests and the reflected electromagnetic wave, and (iv) on the space distance between the reflective elements.

2. The wireless communication device of claim 1, wherein a first group of reflective elements are each associated with a corresponding space-time phase shifter, the control unit being adapted to control each space-time phase shifter to add, to each (q,v)-th element of the first group of reflective elements, the phase delay $\beta_{q,v}(t)$, wherein

$$\beta_{q,v}(t) = \varphi_{q,v} + \gamma\left(t + \Delta t_{q,v}\right)$$

wherein

$$\varphi_{q,v} = \frac{\pi}{2}(q\,(\cos\theta_i \cos\phi_i + \cos\theta_r \cos\phi_r) + v\,(\cos\theta_i \sin\phi_i + \cos\theta_r \sin\phi_r))$$

wherein

$$\Delta t_{q,v} = q d_x \frac{\cos\theta_i \cos\phi_i}{c} + q d_y \frac{\cos\theta_i \sin\phi_i}{c}$$

wherein

d_x is the distance between two consecutive elements in the x direction, d_y is the distance between two consecutive elements in the y direction, θ_i and ϕ_i are the incident angles, θ_r and ϕ_r are the reflection angles.

3. The wireless communication device of claim 1 or 2, wherein a second group of reflective elements are each associated with a corresponding space phase shifter, and wherein all the reflective elements of the second group of reflective elements are associated to a common time phase shifter,

wherein the control unit is configured to control the time phase shifter in order to introduce a time phase delay $\gamma(t)$ equal to or proportional to the additional information to be transmitted,

wherein the control unit is configured to control each space phase shifter in order to introduce a further space phase delay, so that the overall time-space phase delay $\beta_{q,v}(t)$ introduced by the (q,v)-th reflective element of the second group, is

$$\beta_{q,v}(t) = \varphi_{q,v} + \gamma(t) - \gamma^{(1)}(\Delta t_{q,v})$$

wherein $\gamma^{(1)}(t)$ is the first order derivate of $\gamma(t)$,

wherein

$$\varphi_{q,v} = \frac{\pi}{2}(q\,(\cos\theta_i\cos\phi_i + \cos\theta_r\cos\phi_r) + v\,(\cos\theta_i\sin\phi_i + \cos\theta_r\sin\phi_r))$$

wherein $\Delta t_{q,v} = qd_x\frac{\cos\theta_i\cos\phi_i}{c} + qd_y\frac{\cos\theta_i\sin\phi_i}{c}$

wherein d_x is the distance between two consecutive elements in the x direction, d_y is the distance between two consecutive elements in the y direction, θ_i and ϕ_i are the incident angles, θ_r and ϕ_r are the reflection angles.

4. The wireless communication device of claim 1 or 2 or 3, wherein the reflective elements have dimensions lower than the wavelength of the incident electromagnetic wave.

5. The wireless communication device of according to any of the previous claims, further comprising a source of electromagnetic waves configured to generate the incident electromagnetic wave.

6. The wireless communication according to claim 5, wherein the incident electromagnetic waves carries no information.

7. The wireless communication device according to any of the previous claims, wherein the array of reflective elements is a metasurface comprising quasi-passive arrays of sub-wavelength-sized elements whose scattering properties are engineered to manipulate the impinging electromagnetic waves and control the reflection.

8. The wireless communication device according to any of the previous claims, wherein the control unit is further configured to control each reflective element in order to further introduce, in the incident electromagnetic wave that hits the reflective element, and amplitude modulation.

9. A wireless communication device comprising:

- an array (210) of transmitting elements (211) adapted to transmit an incident electromagnetic wave (230), and
- a control unit (220) operatively connected to each transmitting element of the array in order to space-time modulating the incident electromagnetic wave to transmit additional information with the transmitted electromagnetic wave (240),

Wherein the control unit is configured to control each transmitting element in order to introduce, in the incident electromagnetic wave that hits the transmitting element, a phase shift which depends (i) on the additional information to be transmitted, (ii) on the incident angles θ_i and ϕ_i formed between the plane on which the array rests and the incident electromagnetic wave, (iii) on the transmission angles θ_t and ϕ_t formed between the plane on which the array rests and the transmitted electromagnetic wave, and (iv) on the space distance between the transmitting elements.

10. The wireless communication device of claim 9, wherein a first group of transmitting elements are each associated with a corresponding space-time phase shifter, the control unit being adapted to control each space-time phase shifter to add, to each (q,v)-th element of the first group of transmitting elements, the phase delay $\beta_{q,v}(t)$, wherein

$$\beta_{q,v}(t) = \varphi_{q,v} + \gamma\left(t + \Delta t_{q,v}\right)$$

wherein

$$\varphi_{q,v} = \frac{\pi}{2}\left(q\left(\cos\theta_i \cos\phi_i + \cos\theta_t \cos\phi_t\right) + v\left(\cos\theta_i \sin\phi_i + \cos\theta_t \sin\phi_t\right)\right)$$

wherein

$$\Delta t_{q,v} = q d_x \frac{\cos\theta_i \cos\phi_i}{c} + q d_y \frac{\cos\theta_i \sin\phi_i}{c}$$

wherein

d_x is the distance between two consecutive elements in the x direction, d_y is the distance between two consecutive elements in the y direction, θ_i and ϕ_i are the incident angles, θ_t and ϕ_t are the transmission angles.

11. The wireless communication device of claim 10, wherein a second group of transmitting elements are each associated with a corresponding space phase shifter, and wherein all the transmitting elements of the second group of transmitting elements are associated to a common time phase shifter,

wherein the control unit is configured to control the time phase shifter in order to introduce a time phase delay $\gamma(t)$ equal to or proportional to the additional information to be transmitted,

wherein the control unit is configured to control each space phase shifter in order to introduce a further space phase delay, so that the overall time-space phase delay $\beta_{q,v}(t)$ introduced by the (q,v)-th transmitting element of the second group, is

$$\beta_{q,v}(t) = \varphi_{q,v} + \gamma(t) - \gamma^{(1)}\left(\Delta t_{q,v}\right)$$

wherein $\gamma^{(1)}(t)$ is the first order derivate of $\gamma(t)$,

wherein

$$\varphi_{q,v} = \frac{\pi}{2}\left(q\left(\cos\theta_i \cos\phi_i + \cos\theta_t \cos\phi_t\right) + v\left(\cos\theta_i \sin\phi_i + \cos\theta_t \sin\phi_t\right)\right)$$

wherein

$$\Delta t_{q,v} = q d_x \frac{\cos\theta_i \cos\phi_i}{c} + q d_y \frac{\cos\theta_i \sin\phi_i}{c}$$

wherein d_x is the distance between two consecutive elements in the x direction, d_y is the distance between two consecutive elements in the y direction, θ_i and ϕ_i are the incident angles, θ_t and ϕ_t are the transmission angles.

12. The wireless communication device of claim 9 or 10 or 11, wherein the transmitting elements have dimensions lower than the wavelength of the incident electromagnetic wave.

13. The wireless communication device of according to any of claims 9 to 12, further comprising a source of electromagnetic waves configured to generate the incident electromagnetic wave.

14. The wireless communication according to claim 13, wherein the incident electromagnetic waves carries no information.

15. The wireless communication device according to any of claims 9 to 14, wherein the array of transmitting elements is a metasurface comprising quasi-passive arrays of sub-wavelength-sized elements whose scattering properties are engineered to manipulate the impinging electromagnetic waves and control the transmission.

16. The wireless communication device according to any of claims 9 to 15, wherein the control unit is further configured to control each transmitting element in order to further introduce, in the incident electromagnetic wave that hits the transmitting element, and amplitude modulation.

17. A method for transmitting information in a wireless network, comprising the steps of:

- determining the incident angle of an incident electromagnetic wave, the incident electromagnetic wave hitting a plurality of reflecting elements of a reflecting surface,
- determining the reflection angle of a reflected wave, the reflected electromagnetic wave being transmitted by the plurality of reflecting elements being hit by the incident electromagnetic wave,
- acquiring an information to be added to the incident electromagnetic wave, and
- controlling each reflecting element of the reflective surface in order to introduce, in the incident electromagnetic wave that hits the reflective element, a phase (and amplitude) shift which depends (i) on the additional information to be transmitted, (ii) on the incident angles θ_i and ϕ_i formed between the plane on which the array rests and the incident electromagnetic wave, (iii) on the reflection angles θ_r and ϕ_r formed between the plane on which the array rests and the reflected electromagnetic wave, and (iv) on the space distance between the reflective elements.

18. The method of claim 17, wherein a first group of reflective elements are each associated with a corresponding space-time phase shifter, the method providing for

controlling each space-time phase shifter to add, to each q,v-th element of the first group of reflective elements, the phase delay $\beta_{q,v}(t)$, wherein

$$\beta_{q,v}(t) = \varphi_{q,v} + \gamma(t + \Delta t_{q,v})$$

wherein

$$\varphi_{q,v} = \frac{\pi}{2}(q\,(\cos\theta_i \cos\phi_i + \cos\theta_r \cos\phi_r) + v\,(\cos\theta_i \sin\phi_i + \cos\theta_r \sin\phi_r))$$

wherein

$$\Delta t_{q,v} = qd_x \frac{\cos\theta_i \cos\phi_i}{c} + qd_y \frac{\cos\theta_i \sin\phi_i}{c}$$

wherein

d_x is the distance between two consecutive elements in the x direction, d_y is the distance between two consecutive elements in the y direction, θ_i and ϕ_i are the incident angles, θ_r and ϕ_r are the reflection angles.

19. The method of claim 17 or 18, wherein a second group of reflective elements are each associated with a corresponding space phase shifter, and wherein all the reflective elements of the second group of reflective elements are associated to a common time phase shifter,

wherein the method provides for controlling the time phase shifter in order to introduce a time phase delay $\gamma(t)$ equal to or proportional to the additional information to be transmitted,

wherein the method provides for controlling each space phase shifter in order to introduce a further space phase delay, so that the overall time-space phase delay $\beta_{q,v}(t)$ introduced by the q,v-th reflective element of the second group, is

$$\beta_{q,v}(t) = \varphi_{q,v} + \gamma(t) - \gamma^{(1)}(\Delta t_{q,v})$$

wherein $\gamma^{(1)}(t)$ is the first order derivate of $\gamma(t)$,

wherein

$$\varphi_{q,v} = \frac{\pi}{2}(q\,(\cos\theta_i \cos\phi_i + \cos\theta_r \cos\phi_r) + v\,(\cos\theta_i \sin\phi_i + \cos\theta_r \sin\phi_r))$$

wherein $\Delta t_{q,v} = qd_x \frac{\cos\theta_i \cos\phi_i}{c} + qd_y \frac{\cos\theta_i \sin\phi_i}{c}$

wherein d_x is the distance between two consecutive elements in the x direction, d_y is the distance between two consecutive elements in the y direction, θ_i and ϕ_i are the incident angles, θ_r and ϕ_r are the reflection angles.

20. The method of claim 17 or 18 or 19, wherein the reflective elements have dimensions lower than the wavelength of the incident electromagnetic wave.

21. The method according to any of claims 17-20, wherein the incident electromagnetic waves carries no information.

22. The method according to any of claims 17-21, wherein the array of reflective elements is a metasurface comprising quasi-passive arrays of sub-wavelength-sized elements whose scattering properties are engineered to manipulate the impinging electromagnetic waves and control the reflection.

23. A method for transmitting information in a wireless network comprising the steps of:

- determining the incident angle of an incident electromagnetic wave, the incident electromagnetic wave hitting a plurality of transmittive elements of a transmitting surface,
- determining the transmission angle of a transmitted wave, the transmitted electromagnetic wave being transmitted by the plurality of transmitting elements being hit by the incident electromagnetic wave,
- acquiring an information to be added to the incident electromagnetic wave, and
- controlling each transmitting elements of the array in order to modify the phase of the incident electromagnetic wave by adding a phase shift which depends (i) on the information that the control units (120) is requested to add, (ii) on the incident angles θ_i and ϕ_i and the transmission angle θ_t and ϕ_t, (iii) on the space distance between the transmitting elements.

24. The method of claim 17, wherein a first group of reflective elements are each associated with a corresponding space-time phase shifter, the method providing for controlling each space-time phase shifter to add, to each (q,v)-th element of the first group of transmitting elements, the phase delay $\beta_{q,v}(t)$, wherein

$$\beta_{q,v}(t) = \varphi_{q,v} + \gamma\left(t + \Delta t_{q,v}\right)$$

wherein

$$\varphi_{q,v} = \frac{\pi}{2}(q\,(\cos\theta_i \cos\phi_i + \cos\theta_t \cos\phi_t) + v\,(\cos\theta_i \sin\phi_i + \cos\theta_t \sin\phi_t))$$

wherein

$$\Delta t_{q,v} = qd_x \frac{\cos\theta_i \cos\phi_i}{c} + qd_y \frac{\cos\theta_i \sin\phi_i}{c}$$

wherein

d_x is the distance between two consecutive elements in the x direction, d_y is the distance between two consecutive elements in the y direction, θ_i and ϕ_i are the incident angle and θ_t and ϕ_t is the transmission angle.

25. The method of claim 23 or 24, wherein a second group of transmitting elements are each associated with a corresponding space phase shifter, and wherein all the transmitting elements of the second group of transmitting elements are associated to a common time phase shifter,

wherein the method provides for controlling the time phase shifter in order to introduce a time phase delay $\gamma(t)$ equal to or proportional to the additional information to be transmitted,

wherein the method provides for controlling each space phase shifter in order to introduce a further space phase delay, so that the overall time-space phase delay $\beta_{q,v}(t)$ introduced by the (q,v)-th transmittive element of the second group, is

$$\beta_{q,v}(t) = \varphi_{q,v} + \gamma(t) - \gamma^{(1)}(\Delta t_{q,v})$$

wherein $\gamma^{(1)}(\mathrm{t})$ is the first order derivate of $\gamma(t)$,

wherein

$$\varphi_{q,v} = \frac{\pi}{2}(q\,(\cos\theta_i \cos\phi_i + \cos\theta_t \cos\phi_t) + v\,(\cos\theta_i \sin\phi_i + \cos\theta_t \sin\phi_t))$$

wherein $\Delta t_{q,v} = q d_x \frac{\cos\theta_i \cos\phi_i}{c} + q d_y \frac{\cos\theta_i \sin\phi_i}{c}$

wherein d_x is the distance between two consecutive elements in the x direction, d_y is the distance between two consecutive elements in the y direction, θ_i and ϕ_i are the incident angles, θ_t and ϕ_t are the transmission angles.

26. The method of claim 23 or 24 or 25, wherein the transmitting elements have dimensions lower than the wavelength of the incident electromagnetic wave.

27. The method according to any of claims 23-26, wherein the incident electromagnetic waves carries no information.

28. The method according to any of claims 23-27, wherein the array of transmitting elements is a metasurface comprising quasi-passive arrays of sub-wavelength-sized elements whose scattering properties are engineered to manipulate the impinging electromagnetic waves and control the reflection.

29. A wireless communication network comprising at least a wireless communication device according to any of claims 1-16.

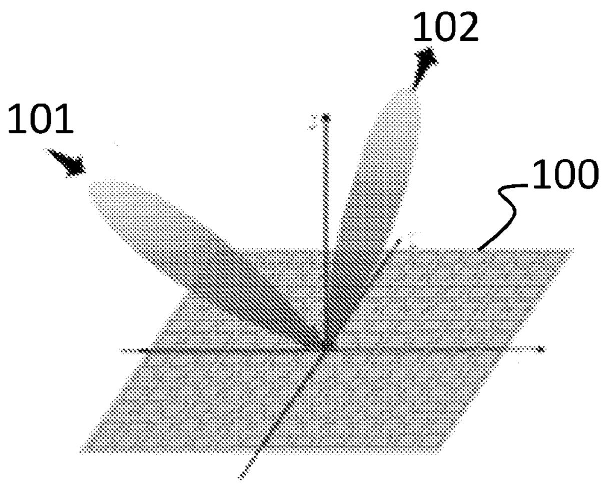

Fig. 1a

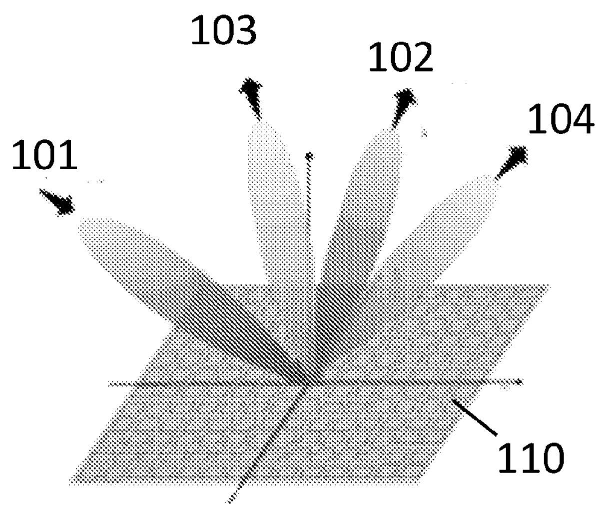

Fig. 1b

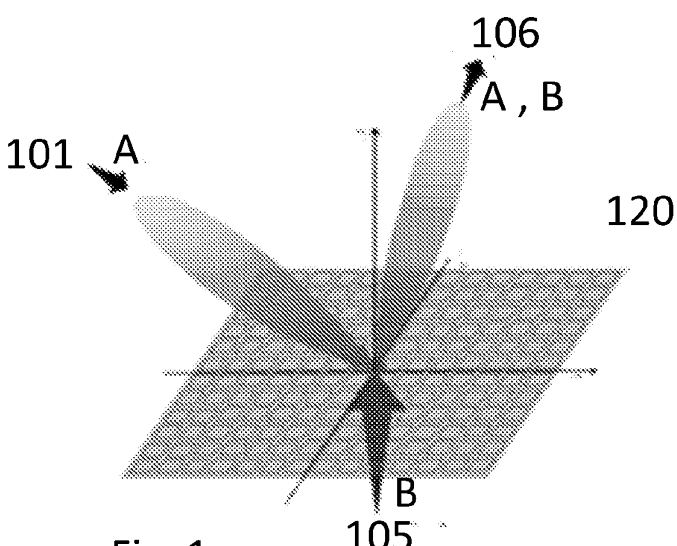

Fig. 1c

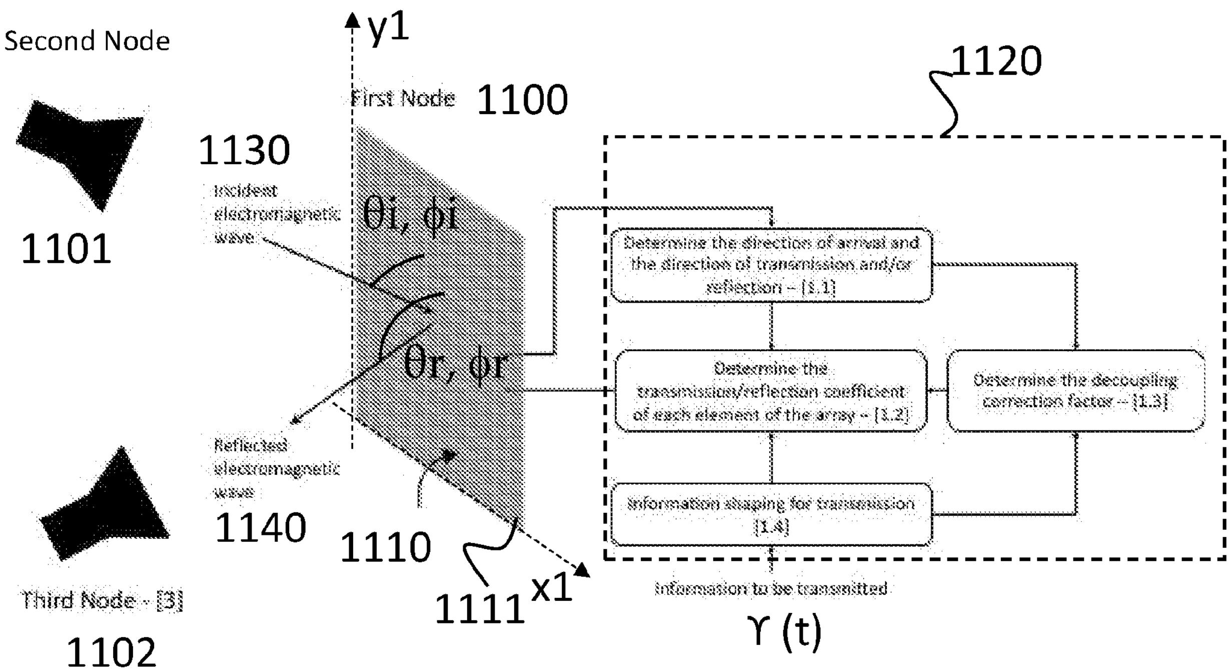

Fig. 2

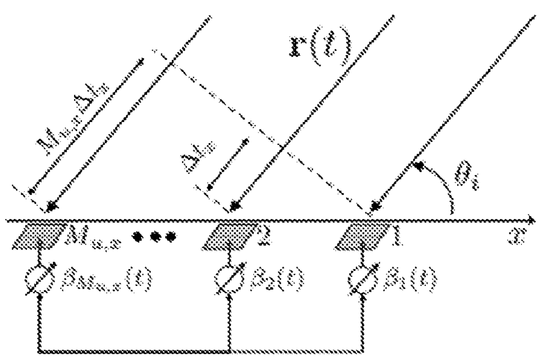

Fig. 3a Architecture A

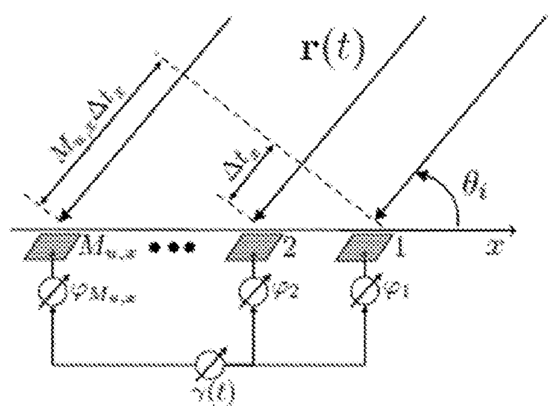

Fig. 3b Architecture B

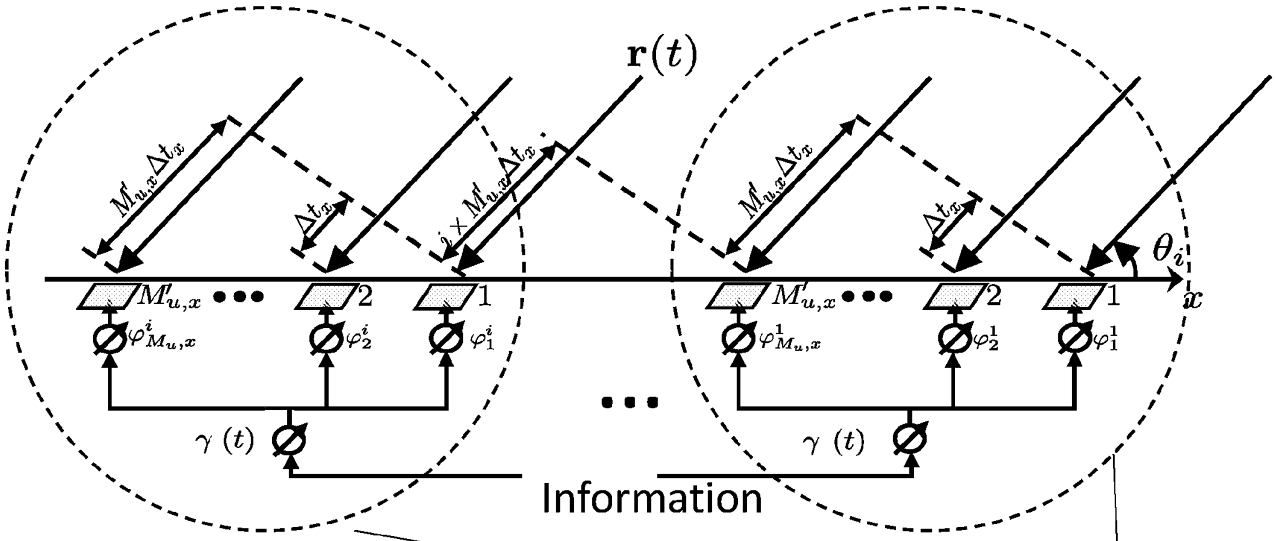

Fig. 4a

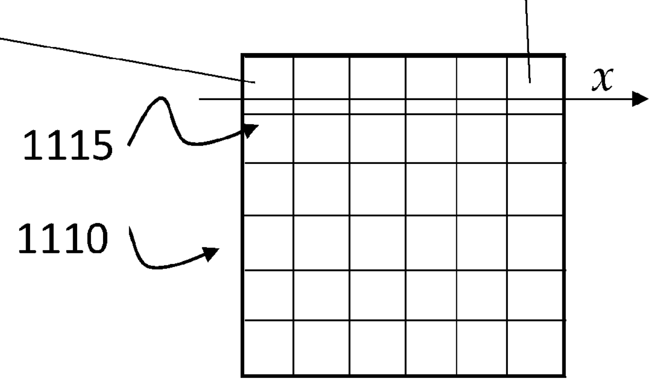

Fig. 4b

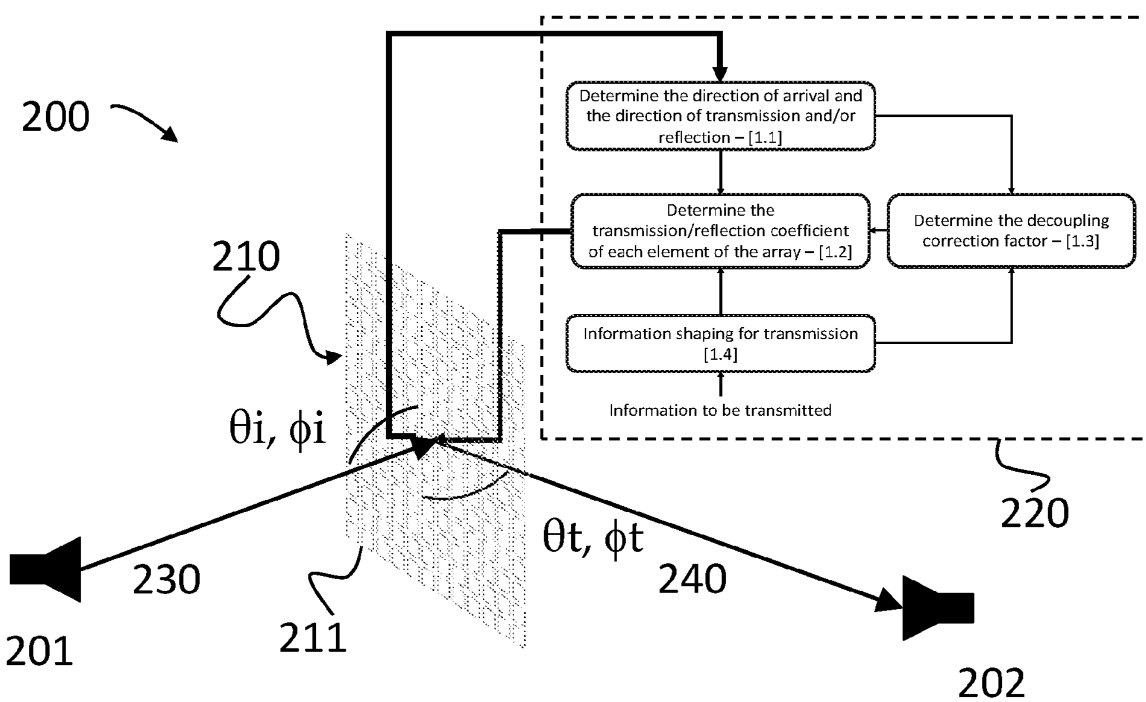

Fig. 5

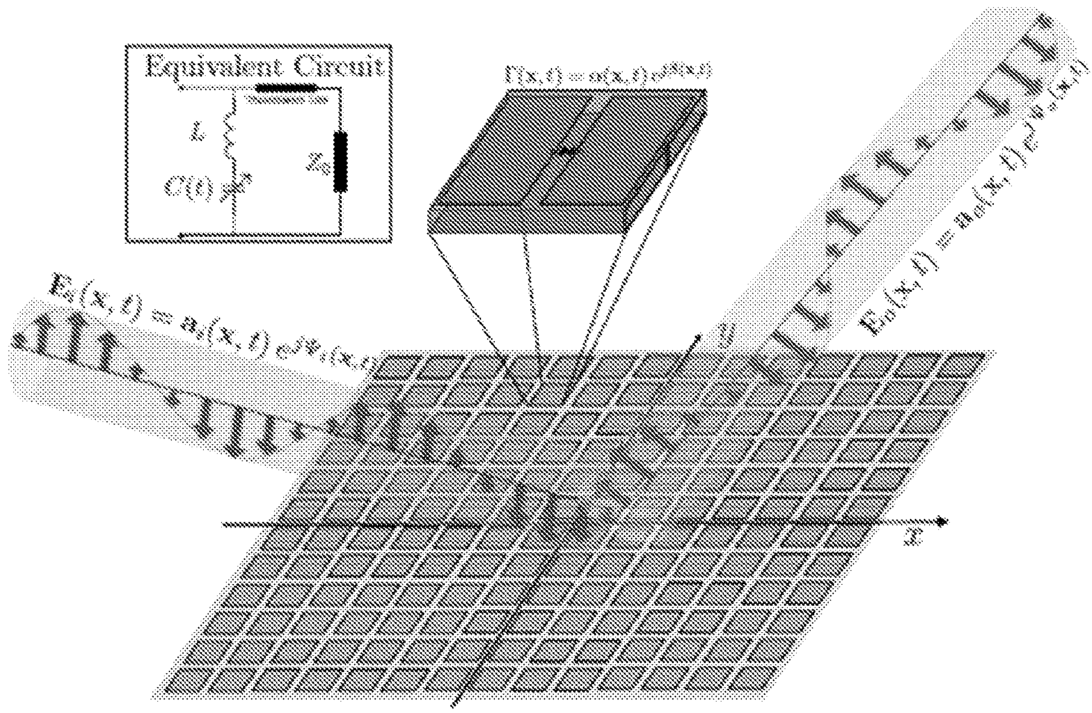

Fig. 6

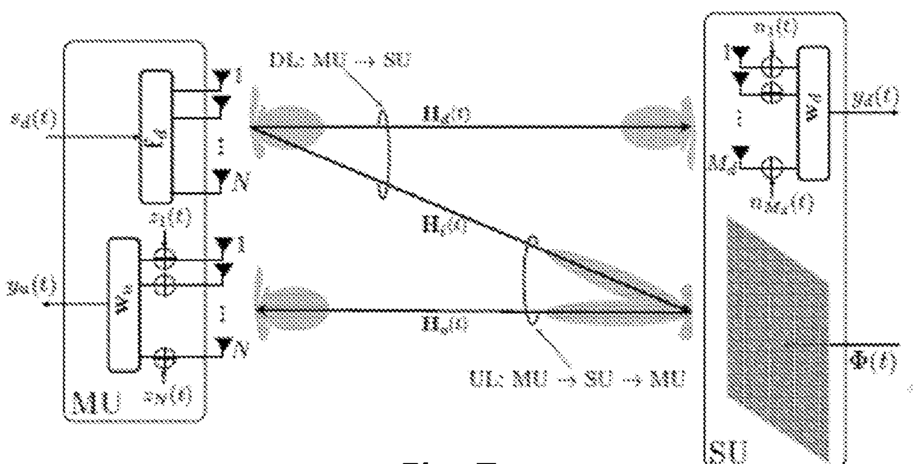

Fig. 7a

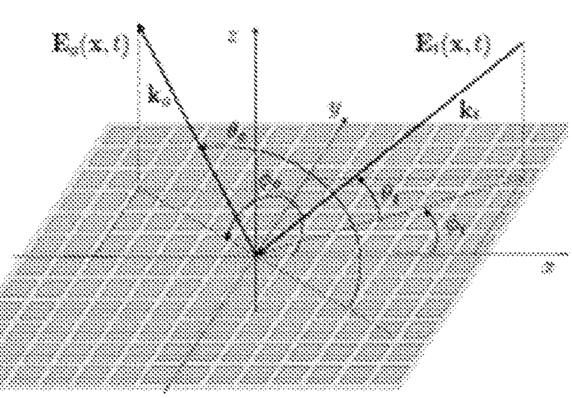

Fig. 7b

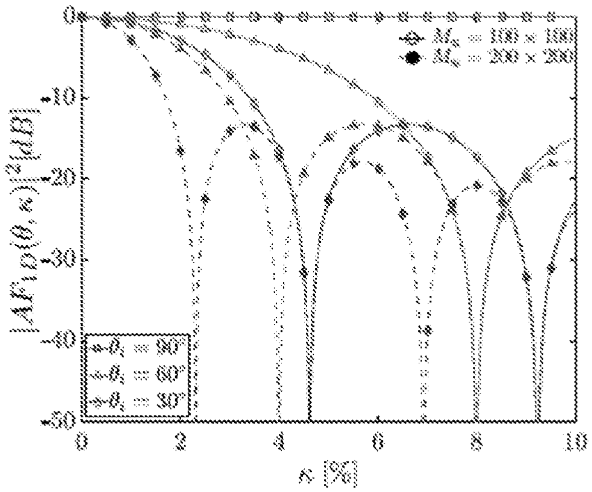

Fig. 8

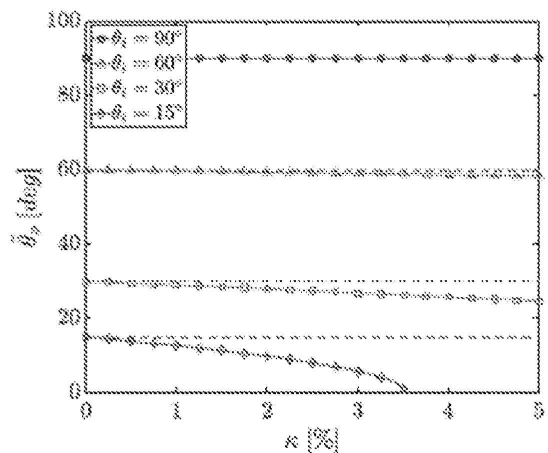

Fig. 9

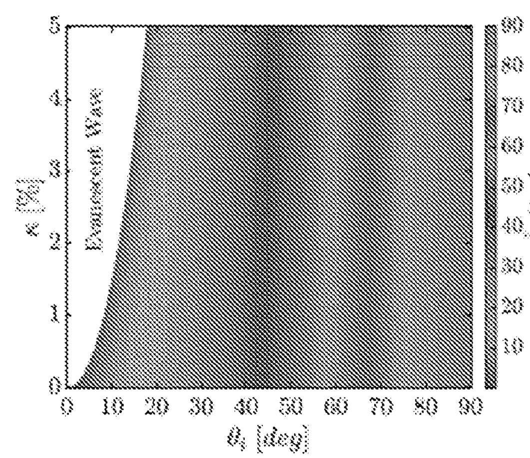

Fig. 10

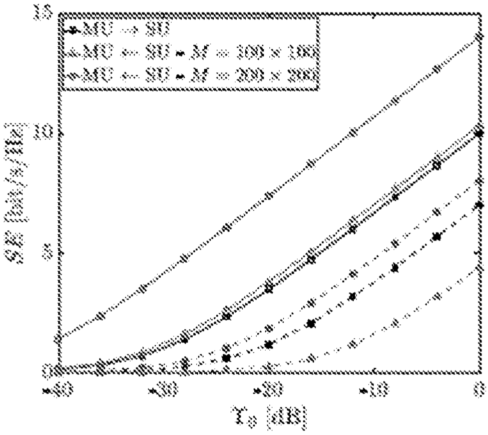

Fig. 11a

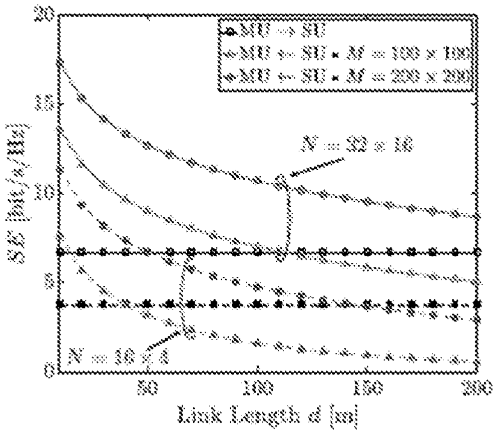

Fig. 11b

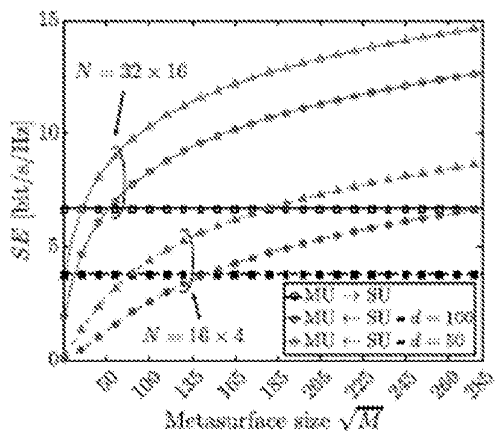

Fig. 11c

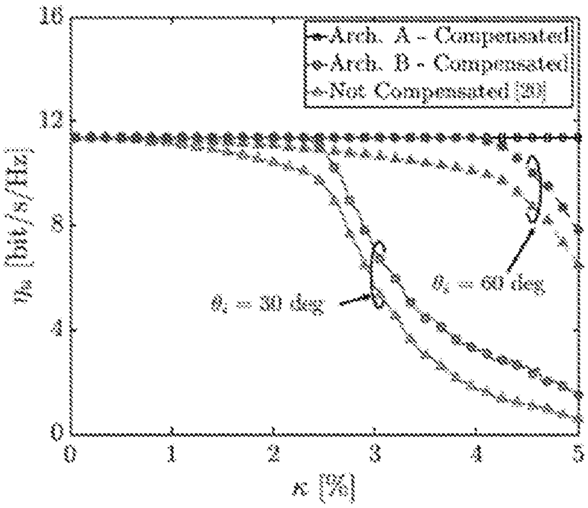

Fig. 12a

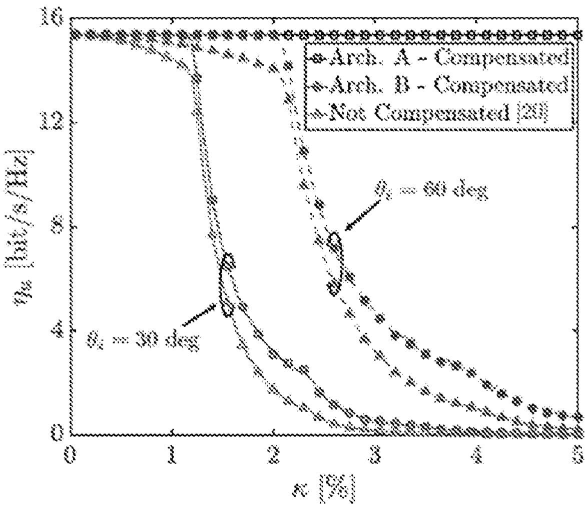

Fig. 12b

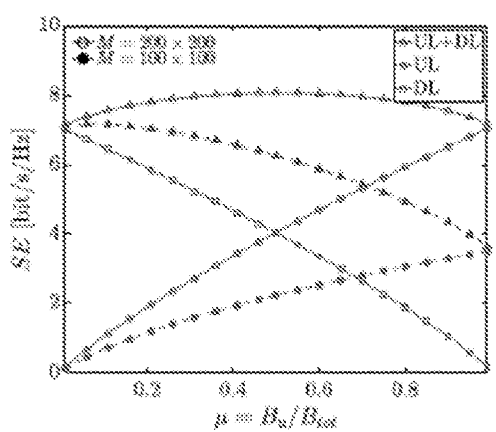

Fig. 13

INTERNATIONAL SEARCH REPORT

International application No
PCT/IB2024/051409

A. CLASSIFICATION OF SUBJECT MATTER
INV. H04B7/04 H04B7/06
ADD.

According to International Patent Classification (IPC) or to both national classification and IPC

B. FIELDS SEARCHED

Minimum documentation searched (classification system followed by classification symbols)
H04B

Documentation searched other than minimum documentation to the extent that such documents are included in the fields searched

Electronic data base consulted during the international search (name of data base and, where practicable, search terms used)

EPO-Internal

C. DOCUMENTS CONSIDERED TO BE RELEVANT

Category*	Citation of document, with indication, where appropriate, of the relevant passages	Relevant to claim No.
X	US 2022/052764 A1 (MEDRA MOSTAFA [CA] ET AL) 17 February 2022 (2022-02-17) paragraph [0007] - paragraph [0008] paragraph [0054] - paragraph [0069] paragraph [0126] - paragraph [0129] figures 1-7 -----	1-29
A	EP 3 962 006 A1 (VESTEL ELEKTRONIK SANAYI VE TICARET AS [TR]) 2 March 2022 (2022-03-02) paragraph [0038] - paragraph [0039] paragraph [0046] - paragraph [0055] figure 4 -----	1-29
A	US 2022/322321 A1 (DAI YUCHENG [US] ET AL) 6 October 2022 (2022-10-06) paragraph [0071] - paragraph [0075] figure 2 -----	1-29

☐ Further documents are listed in the continuation of Box C.

☒ See patent family annex.

* Special categories of cited documents :

"A" document defining the general state of the art which is not considered to be of particular relevance

"E" earlier application or patent but published on or after the international filing date

"L" document which may throw doubts on priority claim(s) or which is cited to establish the publication date of another citation or other special reason (as specified)

"O" document referring to an oral disclosure, use, exhibition or other means

"P" document published prior to the international filing date but later than the priority date claimed

"T" later document published after the international filing date or priority date and not in conflict with the application but cited to understand the principle or theory underlying the invention

"X" document of particular relevance;; the claimed invention cannot be considered novel or cannot be considered to involve an inventive step when the document is taken alone

"Y" document of particular relevance;; the claimed invention cannot be considered to involve an inventive step when the document is combined with one or more other such documents, such combination being obvious to a person skilled in the art

"&" document member of the same patent family

Date of the actual completion of the international search	Date of mailing of the international search report
18 April 2024	07/05/2024

Name and mailing address of the ISA/	Authorized officer
European Patent Office, P.B. 5818 Patentlaan 2 NL - 2280 HV Rijswijk Tel. (+31-70) 340-2040, Fax: (+31-70) 340-3016	Spinnler, Florian

1

INTERNATIONAL SEARCH REPORT

Information on patent family members

International application No
PCT/IB2024/051409

Patent document cited in search report		Publication date	Patent family member(s)			Publication date
US 2022052764	A1	17-02-2022	CN	116114185	A	12-05-2023
			US	2022052764	A1	17-02-2022
			WO	2022033042	A1	17-02-2022
EP 3962006	A1	02-03-2022	CN	116057852	A	02-05-2023
			EP	3962006	A1	02-03-2022
			JP	2023538822	A	12-09-2023
			KR	20230058512	A	03-05-2023
			US	2023421412	A1	28-12-2023
			WO	2022049112	A1	10-03-2022
US 2022322321	A1	06-10-2022	NONE			